

1 **Title:** Alum:CpG adjuvant enables SARS-CoV-2 RBD-induced protection in aged mice and
2 synergistic activation of human elder type 1 immunity

3
4 **One Sentence Summary:** Alum and CpG enhance SARS-CoV-2 RBD protective immunity,
5 variant neutralization in aged mice and Th1-polarizing cytokine production by human elder
6 leukocytes.

7
8 **Authors:** Etsuro Nanishi^{1, 2†}, Francesco Borriello^{1, 2, 3†}, Timothy R. O’Meara^{1‡}, Marisa E.
9 McGrath^{4‡}, Yoshine Saito¹, Robert E. Haupt⁴, Hyuk-Soo Seo^{5, 6}, Simon D. van Haren^{1, 2}, Byron
10 Brook^{1, 2}, Jing Chen⁷, Joann Diray-Arce^{1, 2}, Simon Doss-Gollin¹, Maria De Leon¹, Katherine
11 Chew¹, Manisha Menon¹, Kijun Song⁵, Andrew Z. Xu⁵, Timothy M. Caradonna⁸, Jared
12 Feldman⁸, Blake M. Hauser⁸, Aaron G. Schmidt^{8, 9}, Amy C. Sherman^{1, 10}, Lindsey R. Baden¹⁰,
13 Robert K. Ernst¹¹, Carly Dillen⁴, Stuart M. Weston⁴, Robert M. Johnson⁴, Holly L. Hammond⁴,
14 Romana Mayer¹², Allen Burke¹², Maria E. Bottazzi^{13, 14}, Peter J. Hotez^{13, 14}, Ulrich Strych^{13, 15},
15 Aiquan Chang¹⁶, Jingyou Yu¹⁶, Dan H. Barouch¹⁶, Sirano Dhe-Paganon^{5, 6}, Ivan Zanoni^{2, 3}, Al
16 Ozonoff^{1, 2}, Matthew B. Frieman^{4§}, Ofer Levy^{1, 2, 17§}, David J. Dowling^{1, 2§*}

17
18 **Affiliations:**

19 ¹*Precision Vaccines Program*, Division of Infectious Diseases, Boston Children’s Hospital,
20 Boston, MA, USA.

21 ²Department of Pediatrics, Harvard Medical School, Boston, MA, USA.

22 ³Division of Immunology, Boston Children’s Hospital, Boston, MA, USA.

23 ⁴Department of Microbiology and Immunology, University of Maryland School of Medicine,
24 Baltimore, MD, USA.

25 ⁵Department of Cancer Biology, Dana-Farber Cancer Institute, Boston, MA, USA.

26 ⁶Department of Biological Chemistry and Molecular Pharmacology, Harvard Medical School,
27 Boston, MA, USA.

28 ⁷Research Computing Group, Boston Children's Hospital, Boston, MA, USA.

29 ⁸Ragon Institute of MGH, MIT, and Harvard, Cambridge, MA, USA.

30 ⁹Department of Microbiology, Harvard Medical School, Boston, MA, USA.

31 ¹⁰Department of Medicine, Brigham and Women's Hospital, Boston, MA, USA.

32 ¹¹Department of Microbial Pathogenesis, University of Maryland School of Dentistry, Baltimore,
33 MD, USA.

34 ¹²Department of Pathology, University of Maryland Medical Center, Baltimore, MD, USA.

35 ¹³Texas Children's Hospital Center for Vaccine Development, Baylor College of Medicine,
36 Houston, TX, USA.

37 ¹⁴National School of Tropical Medicine and Departments of Pediatrics and Molecular Virology
38 & Microbiology, Baylor College of Medicine, Houston, TX, USA.

39 ¹⁵National School of Tropical Medicine and Department of Pediatrics, Baylor College of
40 Medicine, Houston, TX, USA.

41 ¹⁶Center for Virology and Vaccine Research, Beth Israel Deaconess Medical Center, Harvard
42 Medical School, Boston, MA, USA.

43 ¹⁷Broad Institute of MIT & Harvard, Cambridge, MA, USA.

44

45 †These authors contributed equally to this manuscript.

46 ‡These authors contributed equally to this manuscript.

47 § Co-senior authors.

48

49 ***Corresponding author:** David J. Dowling, *Precision Vaccines Program*, Division of

50 Infectious Diseases, Boston Children's Hospital; Harvard Medical School, Rm 842, Boston, MA

51 02115, USA. Tel: +1 617-919-6890. e-mail: david.dowling@childrens.harvard.edu

52

53 **ABSTRACT**

54 Global deployment of vaccines that can provide protection across several age groups is still
55 urgently needed to end the COVID-19 pandemic especially for low- and middle-income
56 countries. While vaccines against SARS-CoV-2 based on mRNA and adenoviral-vector
57 technologies have been rapidly developed, additional practical and scalable SARS-CoV-2
58 vaccines are needed to meet global demand. In this context, protein subunit vaccines formulated
59 with appropriate adjuvants represent a promising approach to address this urgent need. Receptor-
60 binding domain (RBD) is a key target of neutralizing antibodies (Abs) but is poorly
61 immunogenic. We therefore compared pattern recognition receptor (PRR) agonists, including
62 those activating STING, TLR3, TLR4 and TLR9, alone or formulated with aluminum hydroxide
63 (AH), and benchmarked them to AS01B and AS03-like emulsion-based adjuvants for their
64 potential to enhance RBD immunogenicity in young and aged mice. We found that the AH and
65 CpG adjuvant formulation (AH:CpG) demonstrated the highest enhancement of anti-RBD
66 neutralizing Ab titers in both age groups (~80-fold over AH), and protected aged mice from the
67 SARS-CoV-2 challenge. Notably, AH:CpG-adjuvanted RBD vaccine elicited neutralizing Abs
68 against both wild-type SARS-CoV-2 and B.1.351 variant at serum concentrations comparable to
69 those induced by the authorized mRNA BNT162b2 vaccine. AH:CpG induced similar cytokine
70 and chemokine gene enrichment patterns in the draining lymph nodes of both young adult and
71 aged mice and synergistically enhanced cytokine and chemokine production in human young
72 adult and elderly mononuclear cells. These data support further development of AH:CpG-
73 adjuvanted RBD as an affordable vaccine that may be effective across multiple age groups.

74

75 **INTRODUCTION**

76 The coronavirus disease 2019 (COVID-19) pandemic caused by severe acute respiratory
77 syndrome coronavirus 2 (SARS-CoV-2) resulted in a serious threat to humanity. Rapid
78 deployment of safe and effective vaccines is proving key to reducing morbidity and mortality of
79 COVID-19, especially in high-risk populations such as the older adults (1). Novel vaccine
80 technologies including mRNA and adenoviral vector vaccines have dramatically accelerated the
81 process of vaccine development, shown high efficacy in preclinical and clinical studies, and
82 therefore been granted Emergency Use Authorization by the Food and Drug Administration (2-9).
83 Unfortunately, worldwide access to these vaccines may be limited by the need for ultra-cold
84 storage (mRNA vaccines), cost, and concerns regarding global scalability especially in the third
85 world (1). This situation not only represents a major ethical problem but may also promote the
86 emergence of vaccine-resistant SARS-CoV-2 strains due to high infection rates in unvaccinated
87 regions (10). Thus, ongoing efforts are needed to investigate additional affordable, easily
88 scalable, and effective vaccine approaches against SARS-CoV-2 to improve global access. To
89 this end, alternative platforms such as inactivated and protein subunit SARS-CoV-2 vaccines
90 have entered different stages of clinical development and in some cases have already been
91 deployed at the population level (11-17). These approaches may play an essential role in the
92 global fight against COVID-19 since they utilize well-established technologies, do not require
93 low temperature storage, and have proven safety and effectiveness in various age groups
94 including young children and the elderly.

95

96 With the exception of inactivated viruses, most SARS-CoV-2 vaccine candidates aim to target
97 the SARS-CoV-2 Spike glycoprotein, as it is required for binding to the human receptor

98 angiotensin-converting enzyme 2 (ACE2) and subsequent cell fusion. In particular, the receptor-
99 binding domain (RBD) of the Spike protein plays a key role in ACE2 binding and is targeted by
100 many neutralizing antibodies (Abs) that exert a protective role against SARS-CoV-2 infection
101 (18-20). RBD is an attractive candidate for a SARS-CoV-2 subunit vaccine and is relatively easy
102 to produce at scale (21, 22); however, it is poorly immunogenic on its own. Structural biology-
103 based vaccine design has been employed to overcome this limitation and has generated
104 encouraging results in preclinical and clinical studies (22-29). A complementary approach to
105 increase the immunogenicity of vaccine antigens consists of using adjuvants, which can enhance
106 antigen immunogenicity by activating receptors of the innate immune system called pattern-
107 recognition receptors (PRRs) and/or modulating antigen pharmacokinetics (30, 31). Adjuvant
108 formulations of aluminum salts and PRR agonists enhance vaccine immune responses compared
109 to aluminum salts or PRR agonists alone (32). AS04 was the first adjuvant system composed of
110 aluminum salts and a PRR agonist, specifically the TLR4 agonist monophosphoryl lipid A
111 (MPLA), to be included in a licensed human papillomavirus and hepatitis B vaccines (32). Thus,
112 combinations of aluminum salts and PRR agonists represent a promising adjuvant platform to
113 enhance RBD immunogenicity.

114
115 Here, we evaluated several combinations of PRR agonists and aluminum hydroxide (AH) and
116 found that the TLR9 agonists CpG oligodeoxynucleotides formulated with AH and RBD
117 dramatically enhanced immune response towards RBD in young mice using a prime-boost
118 immunization schedule. The AH:CpG-adjuvanted RBD vaccine also elicited a robust anti-RBD
119 immune response in aged mice, with the administration of an additional boost dose generating an
120 anti-RBD Ab response comparable to young adult mice and providing complete protection from

121 live SARS-CoV-2 challenge. Overall, our comprehensive, head-to-head adjuvant comparison
122 study demonstrates that AH:CpG co-adjuvantation can overcome both the poor immunogenicity
123 of RBD and immunosenescence, supporting this approach for development of a scalable,
124 affordable, and safe global SARS-CoV-2 vaccine tailored for older adults.

125 **RESULTS**

126 *Evaluation of multiple AH:PRR agonist formulations in young adult mice*

127 We first evaluated whether distinct AH:PRR agonist formulations can overcome the low
128 immunogenicity of monomeric RBD proteins. To this end, we performed a comprehensive
129 comparison of PRR agonists, including 2'3'-cGAMP (stimulator of IFN genes (STING) ligand),
130 Poly (I:C) (TLR3 ligand), PHAD (synthetic MPLA, TLR4 ligand), and CpG-ODN 2395 (TLR9
131 ligand). Each PRR agonist was formulated with and without AH. We also included AS01B (a
132 liposome-based adjuvant containing MPLA and the saponin QS-21) as a clinical-grade
133 benchmark adjuvant with potent immunostimulatory activity. The immunogenicity of vaccine
134 formulations was first evaluated in 3-month-old young adult mice. Mice were immunized
135 intramuscularly twice with 10 µg of monomeric RBD protein formulated with or without
136 adjuvant, in a two-dose prime-boost regimen (Days 0 and 14). Two weeks after the boost
137 immunization, humoral immune responses were evaluated. AH:PRR agonist formulations
138 enhanced both anti-RBD Ab titers and inhibition of RBD binding to human ACE2 (hACE2) as
139 compared to their respective non-AH adjuvanted formulations (**Fig 1A-C**). The Ab response
140 elicited by AH alone was highly skewed to IgG1, with minimal inhibition of hACE2/RBD
141 binding (**Fig 1D, E**). Among various AH:PRR agonist formulations, AH:CpG demonstrated the
142 highest induction of total IgG, IgG1, and IgG2a along with a balanced IgG2a/IgG1 ratio (**Fig**
143 **1A-D**). Furthermore, the AH:CpG formulation significantly enhanced hACE2/RBD binding
144 inhibition compared to all the other AH:PRR agonist formulations (**Fig 1E**). Abs induced by
145 monomeric RBD immunization recognized the native trimeric Spike protein, as demonstrated by
146 a binding ELISA with prefusion stabilized form of spike trimer (**Fig 1F**). To assess long-term
147 immunogenicity, we then evaluated Ab responses and hACE2/RBD binding inhibition on Day

148 210 (**Fig 1G-J**). Of note, AH:CpG formulation maintained high hACE2/RBD binding inhibition
149 while other adjuvant formulations waned their immune responses (**Fig 1E, J**).

150

151 *AH:CpG-formulated RBD vaccine is immunogenic in aged mice*

152 To assess the vaccine response in the context of aging, the immunogenicity of RBD vaccines
153 adjuvanted with AH:PRR agonists was further studied in aged mice (14-month-old). Similar to
154 young mice, the AH:CpG formulation also elicited the highest humoral immune response after
155 prime-boost immunization in aged mice (**Fig 2A-F**). Of note, the vaccine adjuvanted with
156 AH:CpG produced significantly higher hACE2/RBD inhibition and neutralizing titers compared
157 to the vaccine adjuvanted with AS01B, which is known as a potent adjuvant in the human elderly
158 population (33, 34) (**Fig 2E, F**). However, Ab levels were generally lower in aged mice, and the
159 magnitude of the immune response of aged mice receiving the AH:CpG vaccine was
160 significantly lower than that of young mice, suggesting an impaired vaccine response due to
161 immunosenescence in the elderly population (**Fig S1**). To determine whether an additional dose
162 can improve vaccine immunogenicity in aged mice, we administered a second booster dose two
163 weeks after the last immunization. On Day 42 (two weeks after the 2nd boost), enhancement in
164 humoral responses was observed in AH:PRR agonist formulations (**Fig 2G-L**). Notably, a
165 significant enhancement of hACE2/RBD inhibition was observed in aged mice receiving the
166 two-boost AH:CpG vaccination regimen, with inhibition reaching the level of young mice that
167 had received AH:CpG in a prime-boost regimen (**Fig S1**). High serum neutralizing Ab titers
168 were observed in the AH:CpG and AS01B adjuvanted groups after the 2nd boost but not in the
169 non-adjuvanted nor AH alone-adjuvanted RBD groups. Assessment of cytokine production by
170 splenocytes isolated from immunized mice and restimulated *in vitro* with Spike peptides

171 demonstrated high Th1 (IFN γ and IL-2) and low Th2 (IL-4) cytokine production in the AH:CpG
172 and AS01B groups (**Fig 2M**). These results demonstrate that the AH:CpG-adjuvanted RBD
173 vaccine is highly immunogenic in aged mice and an additional booster dose can further enhance
174 anti-RBD humoral responses to match those observed in young mice.

175

176 *AH:CpG-formulated RBD vaccine protects aged mice from lethal viral challenge*

177 Neutralizing Abs are key to protecting from SARS-CoV-2 infection. Since RBD formulated with
178 AH:CpG elicited high titers of neutralizing Abs, we assessed the protection of immunized mice
179 in a challenge model. To this end, we employed the mouse-adapted SARS-CoV-2 MA10 virus
180 strain (35). When tested in young (3-month-old) and aged (14-month-old) BALB/c mice, SARS-
181 CoV-2 MA10 elicited dose-dependent weight loss (**Fig 3A, B**). Notably, aged mice challenged
182 with 10³ PFU or more exhibited dose-dependent mortality by 4 days post-infection (dpi) (**Fig**
183 **3C**). None of the young mice died by 4 dpi, including those that received the highest viral dose,
184 in contrast with aged mice. Next, immunized aged mice were challenged with SARS-CoV-2
185 MA10 six weeks after the second boost. Bodyweight changes were assessed daily up to 4 dpi
186 when the mice were sacrificed for viral titer and histopathology analyses. Aged mice immunized
187 with the AH:CpG and AS01B adjuvanted vaccines showed no weight loss up to 4 dpi, whereas
188 aged mice immunized with non-adjuvanted or AH-adjuvanted RBD showed rapid and significant
189 bodyweight loss of >10% through 4 dpi (**Fig 4A**). Lung tissues were harvested and tested for
190 SARS-CoV-2 viral titer in lung. No detectable live virus in lung tissues was observed in the
191 AH:CpG and AS01B adjuvanted groups, while viral titers were detectable in the vehicle, non-
192 adjuvanted, and AH-adjuvanted groups (**Fig 4B**). Histopathological analysis conducted in lung

193 tissues further confirmed the reduced SARS-CoV-2 infection in aged animals vaccinated with
194 AH:CpG and AS01B adjuvants (**Fig 4C, D**).

195

196 *AH:CpG-formulated RBD and Spike mRNA vaccines elicit comparable levels of neutralizing*
197 *antibodies against wild type SARS-CoV-2 and variants*

198 Recently, it has been reported that SARS-CoV-2 mRNA vaccines are more immunogenic than
199 RBD adjuvanted with oil-in-water emulsions (36). To assess whether this is a general feature of
200 RBD protein vaccines, we used the clinical-grade authorized BNT162b2 Spike mRNA vaccine
201 (Pfizer-BioNTech) as a benchmark and compared it to RBD formulated with AddaS03 (a
202 commercially available version of the oil-in-water emulsion AS03) and to AH:CpG in aged mice.
203 Along with CpG-2395, we also tested CpG-1018, which is included in the Heplisav-B vaccine
204 and has also been tested in combination with Spike/RBD and AH in SARS-CoV-2 studies
205 including human vaccine trials (12, 16, 37). In accordance with previously published data, the
206 mRNA vaccine was highly immunogenic, while RBD formulated with AddaS03 failed to induce
207 significant levels of neutralizing Abs (**Fig 5A-D**). Of note, both AH:CpG formulations elicited
208 levels of anti-RBD (**Fig 5A**), anti-Spike (**Fig 5B**) and neutralizing Abs (**Fig 5C, D**) comparable
209 to or greater than the mRNA vaccine.

210 SARS-CoV-2 variants such as B.1.1.7 and B.1.351 have emerged with reduced
211 neutralization from serum samples of convalescent or vaccinated individuals (38-41). A recent
212 report showed that the mRNA BNT162b2 vaccine maintained its effectiveness against severe
213 COVID-19 with the B.1.351 variant at greater than 90% (42). We therefore evaluated whether
214 RBD + AH:CpG and mRNA BNT162b2 vaccines elicit neutralizing Abs against these variants.
215 As expected, we observed reduced titers against the variants, especially against the B.1.351 (**Fig**

216 **5E**). The neutralization titers of RBD + AH:CpG decreased by 3.2-fold against B.1.351, and the
217 mRNA BNT 162b2 decreased by 6.0-fold. Neutralizing titers against the B.1.351 were
218 comparable between RBD + AH:CpG (GMT 382) and mRNA BNT162b2 (GMT 109).

219

220 *Innate signaling potentiated by AH:CpG formulation is well preserved in aged mice*

221 Lymph nodes (LNs) are critical sites for the interaction between innate and adaptive immune
222 systems and orchestrate the development of vaccine immune responses (43, 44). Specifically,
223 activation of the innate immune system can induce a rapid response in the LN characterized by
224 LN expansion, which is driven by lymphocyte accrual and expression of proinflammatory
225 molecules (45, 46). To gain further insights into the mechanism of action of the AH:CpG
226 formulation, we collected draining LNs (dLNs) 24 hours post injection of AH:CpG or either
227 adjuvant alone. CpG and AH:CpG induced comparable dLN expansion in both age groups (**Fig**
228 **6A**). To characterize the molecular events associated with these treatments further, RNA isolated
229 from dLNs after injection of vehicle, CpG, or AH:CpG was subjected to a quantitative real-time
230 PCR array comprised of 157 genes related to cytokines, chemokines, and type 1 IFN responses.
231 Principal component analysis and hierarchical cluster analysis demonstrated a marked separation
232 between AH and CpG-containing treatments, whereas similar patterns were observed between
233 groups treated with AH:CpG and CpG alone in both age groups (**Fig 6B, C**). Generalized linear
234 model analysis comparing gene expressions after AH, CpG, and AH:CpG treatments further
235 revealed similar gene enrichment patterns between young adult and aged mice (**Fig 6D, E**).
236 These results suggest that CpG and AH:CpG activate similar pathways in young and aged mice
237 to elicit a LN innate response.

238

239 ***AH:CpG synergistically enhances proinflammatory cytokines from human elderly PBMCs***

240 In order to assess the translational relevance of an adjuvant formulation it is key to confirm its
241 ability to activate human immune cells. To this end, we stimulated human peripheral blood
242 mononuclear cells (PBMCs) isolated from young adults (18-40 years old) and elder adults (≥ 65
243 years old) with CpG, AH, and the admixed AH:CpG formulation and measured cytokine and
244 chemokine production. Whereas AH induced limited or no cytokine production, both CpG alone
245 and AH:CpG activated young adult and elderly PBMCs in a concentration-dependent manner
246 (**Fig 7A-D, Fig S2**). PBMCs of both age groups treated with AH:CpG produced significantly
247 higher levels of various proinflammatory cytokines and chemokines than those treated with CpG
248 alone (**Fig 7A-D**). Of note, CpG and AH synergistically induced IL-6, IL-10, TNF, CCL3, and
249 GM-CSF production in both young adult and elderly PBMCs, as defined mathematically (D
250 value, see Methods) (**Fig 7C, D, Fig S2**).

251 **DISCUSSION**

252 The risk of COVID-19-related morbidity and mortality increases with age (47, 48). Currently
253 authorized SARS-CoV-2 vaccines have proven effective at preventing severe COVID-19 (2-4).
254 Nevertheless, there is still the need to develop affordable and accessible vaccines that can
255 provide protection across several age groups, especially for low- and middle-income countries (1,
256 10, 49). Protein subunit vaccines formulated with appropriate adjuvants represent a promising
257 strategy to address this urgent need. Here, we performed a comprehensive head-to-head
258 comparison of multiple adjuvants in age-specific *in vivo* and *ex vivo* animal models, along with
259 age-specific human *in vitro* screening, to determine the appropriate adjuvant for a SARS-CoV-2
260 RBD vaccine in the young and the aged, focusing on the innate and humoral immune response
261 reported to align best with known correlates of protection (50, 51). We found that the AH:CpG
262 adjuvant formulation enhances anti-RBD neutralizing Ab titers and type 1 immunity (i.e. IgG2a
263 switching, Th1 polarization) in both age groups. Aged mice immunized with AH:CpG are
264 protected from live SARS-CoV-2 challenge. Of note, RBD adjuvanted with AH:CpG elicited
265 levels of neutralizing Abs comparable to the clinical-grade BNT162b2 Spike mRNA vaccine.
266 The translational relevance of our findings is also highlighted by the synergistic activation of
267 human PBMCs from older individuals upon stimulation with AH:CpG. Overall, our results
268 expand upon recent preclinical and clinical studies on the enhanced immunogenicity of Spike
269 formulated with AH:CpG by showing that a vaccine composed of RBD and AH:CpG can also
270 induce a robust anti-SARS-CoV-2 immune response across different age groups. Since an RBD
271 antigen is amenable to high-yield manufacturability (52-54), our study also supports the
272 development of RBD formulated with AH:CpG as an affordable and accessible vaccine.
273

274 Among various AH:PRR agonist formulations, AH:CpG elicited the highest immune responses
275 in both young and aged mice. We observed that vaccine immune responses were generally lower
276 in aged mice than in young adult mice, even in the group receiving RBD formulated with
277 AH:CpG. While the lower levels of anti-RBD Abs observed in aged mice are likely sufficient for
278 protection, we found that an additional booster dose in the aged overcame the observed age-
279 dependent reductions in vaccine response and protected aged mice from SARS-CoV-2 challenge.
280 We employed AH, which has been used for >90 years with a firmly established record of safety
281 and efficacy (32) and AS01B, which recently demonstrated excellent adjuvant effects among
282 elderly humans (33, 34), as “benchmarking” adjuvants to compare the exploratory adjuvanted
283 formulations with more established adjuvants. In this context, we demonstrated that the AH:CpG
284 adjuvanted vaccine was superior to a vaccine adjuvanted only with AH and was non-inferior to
285 AS01B. In the context of the aged mice prime-boost setting, AH:CpG-adjuvanted SARS-CoV-2
286 RBD significantly outperformed AS01B with respect to functional anti-RBD inhibition
287 (Geometric mean (GM) with SD, $57 \pm 2\%$ vs. $14 \pm 3\%$) and neutralizing Abs titers (2344 ± 7 vs.
288 117 ± 4).

289
290 In this study, AH:CpG dramatically enhanced vaccine immune responses compared to vaccines
291 adjuvanted with AH or CpG alone in both young and aged mice. AH:PRR agonist formulations
292 have shown promising adjuvanticity in preclinical models, and AS04 (a formulation of
293 aluminum salts and MPLA) is employed in several licensed vaccines (32). While the precise
294 mechanism of action of AH:PRR agonist formulations has not been completely uncovered and is
295 potentially influenced by the degree of adsorption of PRR ligands onto AH, the effects of these
296 formulations are at least in part mediated by enhanced activation of innate immune cells at the

297 injection site (31, 55). In our murine model, we also show that AH:CpG and CpG alone induce
298 comparable proinflammatory gene expression profiles in dLNs. To gain additional mechanistic
299 insight and increase the translational relevance of our findings, we tested the activity of AH:CpG
300 on human PBMCs isolated from young adults and older individuals and found that this adjuvant
301 formulation synergistically enhances cytokine and chemokine production compared to AH or
302 CpG. These results might be explained by either 1) synergistic activation by AH and CpG of
303 distinct molecular pathways, and/or 2) adsorption of CpG onto AH leading to the formation of
304 macromolecular complexes that are more efficiently internalized and/or lead to enhanced TLR9
305 activation. Further work is required to define the underlying molecular mechanism of action of
306 AH:CpG *in vivo* and *in vitro*.

307
308 The rationale for use of a synthetic TLR9 agonist CpG as an adjuvant for SARS-CoV-2 subunit
309 vaccine is multi-fold. First, CpG has been used as a vaccine adjuvant in licensed vaccines with
310 well-known mechanisms, substantial safety data, and confirmed effectiveness (56, 57). Second,
311 CpG has demonstrated adjuvant effects in elderly populations. CpG enhanced vaccinal antigen
312 immunogenicity in aged mouse and porcine models (58-63). Several human trials demonstrated
313 that older individuals had a higher seroprotection rate when immunized with the CpG-adjuvanted
314 hepatitis B vaccine compared to the conventional alum-adjuvanted vaccine (64, 65). Finally,
315 AH:CpG-adjuvanted SARS-CoV-2 Spike vaccines have demonstrated safety, immunogenicity,
316 and efficacy in several young adult animal models (51, 66, 67), and in a human clinical study
317 involving an older population (12). Furthermore, Biological E has recently completed early
318 phase (1 and 2) trials of a AH:CpG-adjuvanted SARS-CoV-2 RBD protein vaccine (trial #
319 CTRI/2020/11/029032) which was intended for low- and middle-income countries, and are

320 currently advancing through manufacturing and clinical development through a large-scale phase
321 3 trial in India (17). CpG is classified into 4 major classes, with distinct activation profiles of
322 human cells (68). Class B CpG-1018 has been extensively evaluated in clinical trials. We
323 observed that CpG-1018 and the class C CpG-2395 formulated with AH elicit comparable levels
324 of neutralizing Abs, resulting in adjuvanted RBD formulations that were both non-inferior to the
325 clinical-grade BNT162b2 Spike mRNA vaccine. Studies of TLR7/8 agonists as precision
326 adjuvants with robust activity in early life (69), including in enhancing Spike immunogenicity in
327 the young (70), further support the use of adjuvants to enhance vaccine immunogenicity in target
328 populations. Together, and in light of our results in the older individuals, these studies suggest
329 that precision adjuvant approaches hold substantial promise to generate scalable adjuvanted
330 SARS-CoV-2 vaccine formulations that do not require freezing and afford robust protection to
331 vulnerable populations across the lifespan.

332
333 Our study features several strengths, including (a) defining a combination adjuvantation system
334 based on the common AH backbone that demonstrated mathematical synergy in its ability to
335 activate human mononuclear cells; (b) accounting for age-specific immunity that can play major
336 roles in vaccine immunogenicity and is often overlooked in vaccine discovery; (c) accounting for
337 species-specificity by assessing the activity of the adjuvant formulation in human PBMCs *in*
338 *vitro* and in mice *in vivo*; (d) testing the ability of the adjuvanted formulation to protect in a
339 SARS-CoV-2 challenge model; and (e) benchmarking to the authorized BNT162b2 Spike
340 mRNA vaccine to place our studies in context. As with any research our study also has some
341 limitations, including that (a) we performed *in vivo* analysis only in mice, establishing the need
342 for future translational research in additional animal models and humans and (b) all

343 adjuvants/antigens were compared in single dose and further analysis should be performed in
344 multiple doses to evaluate both efficacy and reactogenicity. Nevertheless, since we used standard
345 doses of adjuvants/antigens in mouse systems (e.g., 1/30 and 1/18th of the human dose for CpG
346 (12) and BNT162b2 (3) respectively, to compare the CpG-adjuvanted RBD subunit vaccine to
347 the mRNA vaccine), it should be underscored that the results in this study hold promising value
348 from a translational perspective.

349
350 Recently, several SARS-CoV-2 variants of concern have emerged harboring mutations in the
351 RBD region and showing various degrees of reduced neutralization by serum samples obtained
352 from convalescent or vaccinated individuals (38-40). It is likely that booster doses that account
353 for mutations in the Spike protein will be required in order to achieve complete immunity against
354 such variants (71). Several vaccines composed of multiple protein antigens adsorbed onto
355 aluminum salts alone or co-formulated with MPLA have been produced (55, 72). We speculate
356 that an AH:CpG-adjuvanted coronavirus vaccine formulation incorporating RBD proteins from
357 different SARS-CoV-2 strains (and potentially other coronaviruses) may promote cross-strain
358 protective immunity.

359
360 Overall, the current study aimed to evaluate an optimal adjuvant formulation to improve the
361 protective response of RBD-based subunit vaccines in the elderly population, which is otherwise
362 reduced as an effect of aging. We show that an AH:CpG adjuvant formulation induces potent
363 anti-RBD responses in both young and aged mice and overcomes both the poor immunogenicity
364 of the antigen and impaired immune responses in the aged. We discovered unique
365 immunological properties of the AH:CpG adjuvant formulation that demonstrated synergistic

366 enhancement of the production of multiple cytokines and chemokines from human adult and
367 elderly PBMCs *in vitro*. These data indicate that formulating RBD with AH:CpG represents a
368 promising approach to develop a practical (e.g., not requiring low temperature storage), scalable,
369 effective, and affordable vaccine that may be effective across multiple age groups and could
370 potentially incorporate multiple RBD proteins to achieve cross-strain protection.
371

372 **MATERIALS AND METHODS**

373 **Study design.** The aim of this study was to assess optimal combinations of RBD antigen and
374 adjuvants in pre-clinical models that take age-dependent vaccine immune responses and COVID-
375 19 susceptibility into account. To this end, we used age-specific mouse *in vivo* and human *in*
376 *vitro* models. Sample size and age criteria was chosen empirically based on results of previous
377 studies. Mouse experiments aimed to include in total 10 mice per group and were combined from
378 two individual experiments. Mice were randomly assigned to different treatment groups. In order
379 to assess the translational relevance and potential mechanism of an adjuvant formulation, we
380 designed human *in vitro* study with peripheral blood collected from healthy young adults, aged
381 18–40 y (n = 6), and older participants, aged \geq 65 years (n = 6), with approval from the Ethics
382 Committee of the Boston Children’s Hospital (protocol number X07-05-0223) and Institutional
383 Review Board of Brigham and Women’s Hospital, Boston (protocol number 2013P002473). All
384 participants signed an informed consent form prior to enrollment. Investigators were not blinded.
385 No data outliers were excluded.

386
387 **Animals.** Female, 3 months old BALB/c mice were purchased from Jackson Laboratory (Bar
388 Harbor, ME). Female, 12-13 months old BALB/c mice purchased from Taconic Biosciences
389 (Germantown, NY) were used for aged mice experiments. Mice were housed under specific
390 pathogen-free conditions at Boston Children’s Hospital, and all the procedures were approved
391 under the Institutional Animal Care and Use Committee (IACUC) and operated under the
392 supervision of the Department of Animal Resources at Children’s Hospital (ARCH) (Protocol
393 number 19-02-3897R). At the University of Maryland School of Medicine, mice were housed in

394 a biosafety level 3 (BSL3) facility for all SARS-CoV-2 infections with all the procedures
395 approved under the IACUC (Protocol number #1120004) to MBF.
396
397 **SARS-CoV-2 Spike and RBD expression and purification.** Full length SARS-CoV-2 Spike
398 glycoprotein (M1-Q1208, GenBank MN90894) and RBD constructs (amino acid residues R319-
399 K529, GenBank MN975262.1), both with an HRV3C protease cleavage site, a TwinStrepTag
400 and an 8XHisTag at C-terminus were obtained from Barney S. Graham (NIH Vaccine Research
401 Center) and Aaron G. Schmidt (Ragon Institute), respectively. These mammalian expression
402 vectors were used to transfect Expi293F suspension cells (Thermo Fisher) using
403 polyethylenimine (Polysciences). Cells were allowed to grow in 37°C, 8% CO₂ for additional 5
404 days before harvesting for purification. Protein was purified in a PBS buffer (pH 7.4) from
405 filtered supernatants by using either StrepTactin resin (IBA) or Cobalt-TALON resin (Takara).
406 Affinity tags were cleaved off from eluted protein samples by HRV 3C protease, and tag
407 removed proteins were further purified by size-exclusion chromatography using a Superose 6
408 10/300 column (Cytiva) for full length Spike and a Superdex 75 10/300 Increase column
409 (Cytiva) for RBD domain in a PBS buffer (pH 7.4).

410
411 **Adjuvants and immunization.** The adjuvants and their doses used were: Alhydrogel adjuvant
412 2% (100 µg), 2'3'-cGAMP (10 µg), Poly (I:C) HMW (50 µg), CpG-ODN 2395 (50 µg),
413 AddaS03 (25 µL) (all from InvivoGen, San Diego, CA), CpG-ODN 1018 (50 µg, 5' TGA CTG
414 TGA ACG TTC GAG ATG A 3') (Integrated DNA Technologies, Coralville, IA), PHAD (50
415 µg) (Avanti Polar Lipids, Alabaster, AL), and AS01B (40 µL) (obtained from the Shingrix
416 vaccine, GSK Biologicals SA, Belgium). Mice were injected with 10 µg of recombinant

417 monomeric SARS-CoV-2 RBD protein, with or without adjuvants. Each PRR agonist was
418 formulated with and without aluminum hydroxide. Mock treatment mice received phosphate-
419 buffered saline (PBS) alone. BNT162b2 Spike mRNA vaccine (Pfizer-BioNTech) was obtained
420 as residual volumes in used vials from the Boston Children's Hospital employee vaccine clinic,
421 strictly using material that would only otherwise be discarded, and was used within 6 hours from
422 the time of reconstitution. BNT162b2 suspension (100 µg/mL) was diluted 1:3 in PBS, and 50
423 µL (1.67 µg) was injected. Injections (50 µL) were administered intramuscularly in the caudal
424 thigh on Days -0, -14 (both age groups), and Day 28 (aged mice only, where relevant). Blood
425 samples were collected 2 weeks post-immunization.

426
427 **ELISA.** RBD- and Spike-specific antibody levels were quantified in serum samples by ELISA
428 by modification of a previously described protocol(73). Briefly, high-binding flat-bottom 96-well
429 plates (Corning, NY) were coated with 50 ng/well RBD or 25 ng/well Spike and incubated
430 overnight at 4 °C. Plates were washed with 0.05% Tween 20 PBS and blocked with 1% BSA
431 PBS for 1 h at room temperature (RT). Serum samples were serially diluted 4-fold from 1:100 up
432 to 1:1.05E8 and then incubated for 2 hours at RT. Plates were washed three times and incubated
433 for 1 hour at RT with HRP-conjugated anti-mouse IgG, IgG1, IgG2a, or IgG2c (Southern
434 Biotech). Plates were washed five times and developed with tetramethylbenzidine (1-Step Ultra
435 TMB-ELISA Substrate Solution, ThermoFisher, for RBD-ELISA, and BD OptEIA Substrate
436 Solution, BD Biosciences, for Spike ELISA) for 5 min, then stopped with 2 N H₂SO₄. Optical
437 densities (ODs) were read at 450 nm with SpectraMax iD3 microplate reader (Molecular
438 Devices). End-point titers were calculated as the dilution that emitted an optical density

439 exceeding a 3× background. An arbitrary value of 50 was assigned to the samples with OD
440 values below the limit of detection for which it was not possible to interpolate the titer.

441
442 **hACE2/RBD inhibition assay.** The hACE2/RBD inhibition assay employed a modification of a
443 previously published protocol(74). Briefly, high-binding flat-bottom 96-well plates (Corning,
444 NY) were coated with 100 ng/well recombinant human ACE2 (hACE2) (Sigma-Aldrich) in PBS,
445 incubated overnight at 4°C, washed three times with 0.05% Tween 20 PBS, and blocked with
446 1% BSA PBS for 1 hour at RT. Each serum sample was diluted 1:160, pre-incubated with 3 ng
447 of RBD-Fc in 1% BSA PBS for 1 hour at RT, and then transferred to the hACE2-coated plate.
448 RBD-Fc without pre-incubation with serum samples was added as a positive control, and 1%
449 BSA PBS without serum pre-incubation was added as a negative control. Plates were then
450 washed three times and incubated with HRP-conjugated anti-human IgG Fc (Southern Biotech)
451 for 1 hour at RT. Plates were washed five times and developed with tetramethylbenzidine (BD
452 OptEIA Substrate Solution, BD Biosciences) for 5 min, then stopped with 2 N H₂SO₄. The
453 optical density was read at 450 nm with SpectraMax iD3 microplate reader (Molecular Devices).
454 Percentage inhibition of RBD binding to hACE2 was calculated with the following formula:
455 Inhibition (%) = [1 – (Sample OD value – Negative Control OD value)/(Positive Control OD
456 value – Negative Control OD value)] x 100.

457
458 **SARS-CoV-2 neutralization titer determination.** All serum samples were heat-inactivated at
459 56°C for 30 min to remove complement and allowed to equilibrate to RT prior to processing for
460 neutralization titer. Samples were diluted in duplicate to an initial dilution of 1:5 or 1:10
461 followed by 1:2 serial dilutions (vaccinated sample), resulting in a 12-dilution series with each

462 well containing 100 μ L. All dilutions were performed in DMEM (Quality Biological),
463 supplemented with 10% (v/v) fetal bovine serum (heat-inactivated, Sigma), 1% (v/v)
464 penicillin/streptomycin (Gemini Bio-products) and 1% (v/v) L-glutamine (2 mM final
465 concentration, Gibco). Dilution plates were then transported into the BSL-3 laboratory and 100
466 μ L of diluted SARS-CoV-2 (WA-1, courtesy of Dr. Natalie Thornburg/CDC) inoculum was
467 added to each well to result in a multiplicity of infection (MOI) of 0.01 upon transfer to titring
468 plates. A non-treated, virus-only control and mock infection control were included on every plate.
469 The sample/virus mixture was then incubated at 37°C (5.0% CO₂) for 1 hour before transferring
470 to 96-well titer plates with confluent VeroE6 cells. Titer plates were incubated at 37°C (5.0%
471 CO₂) for 72 hours, followed by CPE determination for each well in the plate. The first sample
472 dilution to show CPE was reported as the minimum sample dilution required to neutralize >99%
473 of the concentration of SARS-CoV-2 tested (NT99).

474

475 **Pseudovirus neutralization assay.** The SARS-CoV-2 pseudoviruses expressing a luciferase
476 reporter gene were generated in an approach similar to as described previously (75, 76). Briefly,
477 the packaging plasmid psPAX2 (AIDS Resource and Reagent Program), luciferase reporter
478 plasmid pLenti-CMV Puro-Luc (Addgene), and spike protein expressing pcDNA3.1-SARS
479 CoV-2 S Δ CT of variants were co-transfected into HEK293T cells by lipofectamine 2000
480 (ThermoFisher). Pseudoviruses of SARS-CoV-2 variants were generated by using WA1/2020
481 strain (Wuhan/WIV04/2019, GISAID accession ID: EPI_ISL_402124), B.1.1.7 variant (GISAID
482 accession ID: EPI_ISL_601443), or B.1.351 variant (GISAID accession ID: EPI_ISL_712096).
483 The supernatants containing the pseudotype viruses were collected 48 h post-transfection, which
484 were purified by centrifugation and filtration with 0.45 μ m filter. To determine the neutralization

485 activity of the plasma or serum samples from participants, HEK293T-hACE2 cells were seeded
486 in 96-well tissue culture plates at a density of 1.75×10^4 cells/well overnight. Three-fold serial
487 dilutions of heat inactivated serum or plasma samples were prepared and mixed with 50 μ L of
488 pseudovirus. The mixture was incubated at 37°C for 1 h before adding to HEK293T-hACE2 cells.
489 48 h after infection, cells were lysed in Steady-Glo Luciferase Assay (Promega) according to the
490 manufacturer's instructions. SARS-CoV-2 neutralization titers were defined as the sample
491 dilution at which a 50% reduction in relative light unit (RLU) was observed relative to the
492 average of the virus control wells.

493
494 **Splenocyte restimulation assay.** Immunized mice were sacrificed 2 weeks after the final
495 immunization, and spleens were collected. To isolate splenocytes, spleens were mashed through
496 a 70 μ m cell strainer, and the resulting cell suspensions were washed with PBS and incubated
497 with 2 mL of ACK lysis buffer (Gibco) for 2 minutes at RT to lyse erythrocytes. Splenocytes
498 were washed again with PBS and plated in flat-bottom 96-well plates (2×10^6 cells per well).
499 Then, SARS-CoV-2 Spike peptides (PepTivator SARS-CoV-2 Prot_S, Miltenyi Biotec) were
500 added at a final concentration of 0.6 nmol/ml in the presence of 1 μ g/mL anti-CD28 antibody
501 (total cell culture volume, 200 μ L per well). After 24 (for IL-2 and IL-4) and 96 (for IFN γ) hours,
502 supernatants were harvested, and cytokine levels were measured by ELISA (Invitrogen)
503 according to the manufacturer's protocol.

504
505 **SARS-CoV-2 mouse challenge study.** Mice were anesthetized by intraperitoneal injection 50
506 μ L of a mix of xylazine (0.38 mg/mouse) and ketamine (1.3 mg/mouse) diluted in PBS. Mice
507 were then intranasally inoculated with 1×10^3 PFU of mouse-adapted SARS-CoV-2 (MA10,

508 courtesy of Dr. Ralph Baric (UNC)) in 50 μ L divided between nares(35). Different doses of
509 SARS-CoV-2 were used where indicated. Challenged mice were weighed on the day of infection
510 and daily for up to 4 days post-infection. At 4-day post-infection, mice were sacrificed, and lungs
511 were harvested to determine virus titer by a plaque assay and prepared for histological scoring.

512
513 **SARS-CoV-2 plaque assay.** SARS-CoV-2 lung titers were quantified by homogenizing
514 harvested lungs in PBS (Quality Biological Inc.) using 1.0 mm glass beads (Sigma Aldrich) and
515 a Beadruptor (Omni International Inc.). Homogenates were added to Vero E6 cells and SARS-
516 CoV-2 virus titers determined by counting plaque-forming units (pfu) using a 6-point dilution
517 curve.

518
519 **Histopathology analysis.** Slides were prepared as 5- μ m sections and stained with hematoxylin
520 and eosin. A pathologist was blinded to information identifying the treatment groups and fields
521 were examined by light microscopy and analyzed. The severity of interstitial inflammation was
522 evaluated and converted to a score of 0-4 with 0 being no inflammation and 4 being most severe.
523 Interstitial inflammation was evaluated for the number of neutrophils present in the interstitial
524 space as well as the extent of neutrophilic apoptosis. Once scoring was complete, scores for each
525 group were averaged and the standard deviation for the scoring was computed.

526
527 **Mouse *in vivo* LNs gene expression analysis by quantitative real-time PCR array.** Mice were
528 subcutaneously injected on Day 0 with the indicated treatments in a volume of 50 μ L on each
529 side of the back (one side for the compound and the contralateral side for saline of vehicle
530 control). Twenty-four hours post-injection, draining (brachial) LNs were collected for

531 subsequent analysis. LNs were transferred to a beadbeater and homogenized in TRI Reagent
532 (Zymo Research). Samples were then centrifuged, and the clear supernatant was transferred to a
533 new tube for subsequent RNA isolation. RNA was isolated from TRI Reagent samples using
534 phenol-chloroform extraction or column-based extraction systems (Direct-zol RNA Miniprep,
535 Zymo Research) according to the manufacturer's protocol. RNA concentration and purity
536 (260/280 and 260/230 ratios) were measured by NanoDrop (ThermoFisher Scientific). cDNA
537 was prepared from RNA with RT² First Strand Kit, according to the manufacturer's instructions
538 (Qiagen). cDNA was quantified using 96-well PCR array analysis on a PAMM-150ZA plate
539 (Cytokines & Chemokines) and PAMM-016ZA plate (Type I Interferon Response) (both
540 Qiagen). Quantitative real time-PCR (QRT-PCR) was run on a 7300 real-time PCR system
541 (Applied Biosystems – Life Technologies, Carlsbad, CA). mRNA levels were normalized to 3
542 housekeeping genes: *Actb*, *Gapdh*, and *Gusb*. Relative quantification of gene expression was
543 calculated by the $\Delta\Delta C_t$ (relative expression over PBS treatment group).

544

545 **Human PBMC isolation.** PBMCs were isolated based previously described protocols (77).
546 Briefly, heparinized whole blood was centrifuged at 500 g for 10 min, then the upper layer of
547 platelet-rich plasma was removed. Plasma was centrifuged at 3000 g for 10 min, and platelet-
548 poor plasma (PPP) was collected and stored on ice. The remaining blood was reconstituted to its
549 original volume with heparinized DPBS and layered on Ficoll-Paque gradients (Cytiva) in
550 Accuspin tubes (Sigma-Aldrich). PBMCs were collected after centrifugation and washed twice
551 with PBS.

552

553 **Human PBMCs stimulation.** PBMCs were resuspended at a concentration of 200,000 cells per
554 well in a 96-well U-bottom plate (Corning) in 200 μ L RPMI 1640 media (Gibco) supplemented
555 with 10% autologous PPP, 100 IU/mL penicillin, 100 μ g/mL streptomycin, and 2 mM L-
556 glutamine. PBMCs were incubated for 24 hrs at 37°C in a humidified incubator at 5% CO₂ with
557 indicated treatments. After culture, plates were centrifuged at 500 g and supernatants were
558 removed by pipetting without disturbing the cell pellet. Cytokine expression profiles in cell
559 culture supernatants were measured using customized Milliplex human cytokine magnetic bead
560 panels (Milliplex). Assays were analyzed on the Luminex FLEXMAP 3D employing xPONENT
561 software (Luminex) and Millipore Milliplex Analyst. Cytokine measurements were excluded
562 from analysis if fewer than 30 beads were recovered. Synergy was evaluated using the Loewe
563 definition of additivity, with $D > 1$ indicating antagonism, $D = 1$ additivity, and $D < 1$ synergy
564 (78). In order to fit regression curves more closely to the data, higher concentrations were
565 excluded from linear regressions when calculating D values if the cytokine levels plateaued or
566 decreased.

567
568 **Statistical analysis.** Statistical analyses were performed using Prism v9.0.2 (GraphPad
569 Software) and R software environment v4.0.4. *P* values < 0.05 were considered significant. Data
570 were analyzed by one- or two-way ANOVAs followed by post-hoc Tukey's test or Dunnett's test
571 for multiple comparisons. Non-normally distributed data were log-transformed. In the animal
572 experiences, time to event were analyzed using Kaplan-Meier estimates and compared across
573 groups using the Log-rank test. For human in vitro PBMC assay, unpaired Mann-Whitney tests
574 were applied at each concentration. We conducted gene expression analyses with R 4.0.4 using
575 packages 'ggplot2', 'dplyr', and 'MASS' for the transcript abundance determination of gene

576 arrays in each group. We log-transformed data before performing principal component analysis
577 (PCA) and unsupervised hierarchical clustering using R packages ‘prcomp’ and ‘pheatmap’
578 respectively. We analyzed the differential gene expression using generalized linear models
579 (GLMs) with treatment and age as fixed effects. We then enriched the differentially expressed
580 genes using the blood transcriptional module method based on an existing protocol (Li et al.,
581 2013- PMC: 24336226).
582

583 **REFERENCES**

- 584 1. W. C. Koff, T. Schenkelberg, T. Williams, R. S. Baric, A. McDermott, C. M. Cameron,
585 M. J. Cameron, M. B. Friemann, G. Neumann, Y. Kawaoka, A. A. Kelvin, T. M. Ross, S.
586 Schultz-Cherry, T. D. Mastro, F. H. Priddy, K. A. Moore, J. T. Ostrowsky, M. T.
587 Osterholm, J. Goudsmit, Development and deployment of COVID-19 vaccines for those
588 most vulnerable. *Science Translational Medicine* **13**, eabd1525 (2021).
- 589 2. L. R. Baden, H. M. El Sahly, B. Essink, K. Kotloff, S. Frey, R. Novak, D. Diemert, S. A.
590 Spector, N. Rouphael, C. B. Creech, J. McGettigan, S. Kehtan, N. Segall, J. Solis, A.
591 Brosz, C. Fierro, H. Schwartz, K. Neuzil, L. Corey, P. Gilbert, H. Janes, D. Follmann, M.
592 Marovich, J. Mascola, L. Polakowski, J. Ledgerwood, B. S. Graham, H. Bennett, R.
593 Pajon, C. Knightly, B. Leav, W. Deng, H. Zhou, S. Han, M. Ivarsson, J. Miller, T. Zaks,
594 Efficacy and Safety of the mRNA-1273 SARS-CoV-2 Vaccine. *The New England*
595 *journal of medicine*, (2020).
- 596 3. F. P. Polack, S. J. Thomas, N. Kitchin, J. Absalon, A. Gurtman, S. Lockhart, J. L. Perez,
597 G. Pérez Marc, E. D. Moreira, C. Zerbini, R. Bailey, K. A. Swanson, S. Roychoudhury,
598 K. Koury, P. Li, W. V. Kalina, D. Cooper, R. W. Frenck, Jr., L. L. Hammitt, Ö. Türeci, H.
599 Nell, A. Schaefer, S. Ünal, D. B. Tresnan, S. Mather, P. R. Dormitzer, U. Şahin, K. U.
600 Jansen, W. C. Gruber, Safety and Efficacy of the BNT162b2 mRNA Covid-19 Vaccine.
601 *The New England journal of medicine* **383**, 2603-2615 (2020).
- 602 4. J. Sadoff, M. Le Gars, G. Shukarev, D. Heerwegh, C. Truyers, A. M. de Groot, J. Stoop,
603 S. Tete, W. Van Damme, I. Leroux-Roels, P. J. Berghmans, M. Kimmel, P. Van Damme,
604 J. de Hoon, W. Smith, K. E. Stephenson, S. C. De Rosa, K. W. Cohen, M. J. McElrath, E.
605 Cormier, G. Scheper, D. H. Barouch, J. Hendriks, F. Struyf, M. Douoguih, J. Van Hoof,

- 606 H. Schuitemaker, Interim Results of a Phase 1-2a Trial of Ad26.COV2.S Covid-19
607 Vaccine. *The New England journal of medicine*, (2021).
- 608 5. K. S. Corbett, D. K. Edwards, S. R. Leist, O. M. Abiona, S. Boyoglu-Barnum, R. A.
609 Gillespie, S. Himansu, A. Schäfer, C. T. Ziwawo, A. T. DiPiazza, K. H. Dinnon, S. M.
610 Elbashir, C. A. Shaw, A. Woods, E. J. Fritch, D. R. Martinez, K. W. Bock, M. Minai, B.
611 M. Nagata, G. B. Hutchinson, K. Wu, C. Henry, K. Bahl, D. Garcia-Dominguez, L. Ma, I.
612 Renzi, W. P. Kong, S. D. Schmidt, L. Wang, Y. Zhang, E. Phung, L. A. Chang, R. J.
613 Loomis, N. E. Altaras, E. Narayanan, M. Metkar, V. Presnyak, C. Liu, M. K. Louder, W.
614 Shi, K. Leung, E. S. Yang, A. West, K. L. Gully, L. J. Stevens, N. Wang, D. Wrapp, N. A.
615 Doria-Rose, G. Stewart-Jones, H. Bennett, G. S. Alvarado, M. C. Nason, T. J. Ruckwardt,
616 J. S. McLellan, M. R. Denison, J. D. Chappell, I. N. Moore, K. M. Morabito, J. R.
617 Mascola, R. S. Baric, A. Carfi, B. S. Graham, SARS-CoV-2 mRNA vaccine design
618 enabled by prototype pathogen preparedness. *Nature* **586**, 567-571 (2020).
- 619 6. K. S. Corbett, B. Flynn, K. E. Foulds, J. R. Francica, S. Boyoglu-Barnum, A. P. Werner,
620 B. Flach, S. O'Connell, K. W. Bock, M. Minai, B. M. Nagata, H. Andersen, D. R.
621 Martinez, A. T. Noe, N. Douek, M. M. Donaldson, N. N. Nji, G. S. Alvarado, D. K.
622 Edwards, D. R. Flebbe, E. Lamb, N. A. Doria-Rose, B. C. Lin, M. K. Louder, S. O'Dell,
623 S. D. Schmidt, E. Phung, L. A. Chang, C. Yap, J. M. Todd, L. Pessaint, A. Van Ry, S.
624 Browne, J. Greenhouse, T. Putman-Taylor, A. Strasbaugh, T. A. Campbell, A. Cook, A.
625 Dodson, K. Steingrebe, W. Shi, Y. Zhang, O. M. Abiona, L. Wang, A. Pegu, E. S. Yang,
626 K. Leung, T. Zhou, I. T. Teng, A. Widge, I. Gordon, L. Novik, R. A. Gillespie, R. J.
627 Loomis, J. I. Moliva, G. Stewart-Jones, S. Himansu, W. P. Kong, M. C. Nason, K. M.
628 Morabito, T. J. Ruckwardt, J. E. Ledgerwood, M. R. Gaudinski, P. D. Kwong, J. R.

- 629 Mascola, A. Carfi, M. G. Lewis, R. S. Baric, A. McDermott, I. N. Moore, N. J. Sullivan,
630 M. Roederer, R. A. Seder, B. S. Graham, Evaluation of the mRNA-1273 Vaccine against
631 SARS-CoV-2 in Nonhuman Primates. *The New England journal of medicine* **383**, 1544-
632 1555 (2020).
- 633 7. A. B. Vogel, I. Kanevsky, Y. Che, K. A. Swanson, A. Muik, M. Vormehr, L. M. Kranz,
634 K. C. Walzer, S. Hein, A. Güler, J. Loschko, M. S. Maddur, A. Ota-Setlik, K. Tompkins,
635 J. Cole, B. G. Lui, T. Ziegenhals, A. Plaschke, D. Eisel, S. C. Dany, S. Fesser, S. Erbar, F.
636 Bates, D. Schneider, B. Jesionek, B. Sängler, A. K. Wallisch, Y. Feuchter, H. Junginger, S.
637 A. Krumm, A. P. Heinen, P. Adams-Quack, J. Schlereth, S. Schille, C. Kröner, R. de la
638 Caridad Güimil Garcia, T. Hiller, L. Fischer, R. S. Sellers, S. Choudhary, O. Gonzalez, F.
639 Vascotto, M. R. Gutman, J. A. Fontenot, S. Hall-Ursone, K. Brasky, M. C. Griffor, S.
640 Han, A. A. H. Su, J. A. Lees, N. L. Nedoma, E. H. Mashalidis, P. V. Sahasrabudhe, C. Y.
641 Tan, D. Pavliakova, G. Singh, C. Fontes-Garfias, M. Pride, I. L. Scully, T. Ciolino, J.
642 Obregon, M. Gazi, R. Carrion, Jr., K. J. Alfson, W. V. Kalina, D. Kaushal, P. Y. Shi, T.
643 Klamp, C. Rosenbaum, A. N. Kuhn, Ö. Türeci, P. R. Dormitzer, K. U. Jansen, U. Sahin,
644 BNT162b vaccines protect rhesus macaques from SARS-CoV-2. *Nature* **592**, 283-289
645 (2021).
- 646 8. N. B. Mercado, R. Zahn, F. Wegmann, C. Loos, A. Chandrashekar, J. Yu, J. Liu, L. Peter,
647 K. McMahan, L. H. Tostanoski, X. He, D. R. Martinez, L. Rutten, R. Bos, D. van Manen,
648 J. Vellinga, J. Custers, J. P. Langedijk, T. Kwaks, M. J. G. Bakkers, D. Zuijdsgeest, S. K.
649 Rosendahl Huber, C. Atyeo, S. Fischinger, J. S. Burke, J. Feldman, B. M. Hauser, T. M.
650 Caradonna, E. A. Bondzie, G. Dagotto, M. S. Gebre, E. Hoffman, C. Jacob-Dolan, M.
651 Kirilova, Z. Li, Z. Lin, S. H. Mahrokhian, L. F. Maxfield, F. Nampanya, R. Nityanandam,

- 652 J. P. Nkolola, S. Patel, J. D. Ventura, K. Verrington, H. Wan, L. Pessaint, A. Van Ry, K.
653 Blade, A. Strasbaugh, M. Cabus, R. Brown, A. Cook, S. Zouantchangadou, E. Teow, H.
654 Andersen, M. G. Lewis, Y. Cai, B. Chen, A. G. Schmidt, R. K. Reeves, R. S. Baric, D. A.
655 Lauffenburger, G. Alter, P. Stoffels, M. Mammen, J. Van Hoof, H. Schuitemaker, D. H.
656 Barouch, Single-shot Ad26 vaccine protects against SARS-CoV-2 in rhesus macaques.
657 *Nature* **586**, 583-588 (2020).
- 658 9. M. S. Gebre, L. A. Brito, L. H. Tostanoski, D. K. Edwards, A. Carfi, D. H. Barouch,
659 Novel approaches for vaccine development. *Cell* **184**, 1589-1603 (2021).
- 660 10. I. T. Katz, R. Weintraub, L. G. Bekker, A. M. Brandt, From Vaccine Nationalism to
661 Vaccine Equity - Finding a Path Forward. *The New England journal of medicine* **384**,
662 1281-1283 (2021).
- 663 11. C. Keech, G. Albert, I. Cho, A. Robertson, P. Reed, S. Neal, J. S. Plested, M. Zhu, S.
664 Cloney-Clark, H. Zhou, G. Smith, N. Patel, M. B. Frieman, R. E. Haupt, J. Logue, M.
665 McGrath, S. Weston, P. A. Piedra, C. Desai, K. Callahan, M. Lewis, P. Price-Abbott, N.
666 Formica, V. Shinde, L. Fries, J. D. Lickliter, P. Griffin, B. Wilkinson, G. M. Glenn,
667 Phase 1-2 Trial of a SARS-CoV-2 Recombinant Spike Protein Nanoparticle Vaccine. *The*
668 *New England journal of medicine* **383**, 2320-2332 (2020).
- 669 12. P. Richmond, L. Hatchuel, M. Dong, B. Ma, B. Hu, I. Smolenov, P. Li, P. Liang, H. H.
670 Han, J. Liang, R. Clemens, Safety and immunogenicity of S-Trimer (SCB-2019), a
671 protein subunit vaccine candidate for COVID-19 in healthy adults: a phase 1, randomised,
672 double-blind, placebo-controlled trial. *Lancet (London, England)*, (2021).
- 673 13. S. Xia, Y. Zhang, Y. Wang, H. Wang, Y. Yang, G. F. Gao, W. Tan, G. Wu, M. Xu, Z.
674 Lou, W. Huang, W. Xu, B. Huang, H. Wang, W. Wang, W. Zhang, N. Li, Z. Xie, L. Ding,

- 675 W. You, Y. Zhao, X. Yang, Y. Liu, Q. Wang, L. Huang, Y. Yang, G. Xu, B. Luo, W.
676 Wang, P. Liu, W. Guo, X. Yang, Safety and immunogenicity of an inactivated SARS-
677 CoV-2 vaccine, BBIBP-CorV: a randomised, double-blind, placebo-controlled, phase 1/2
678 trial. *Lancet Infect Dis* **21**, 39-51 (2021).
- 679 14. Y. Zhang, G. Zeng, H. Pan, C. Li, Y. Hu, K. Chu, W. Han, Z. Chen, R. Tang, W. Yin, X.
680 Chen, Y. Hu, X. Liu, C. Jiang, J. Li, M. Yang, Y. Song, X. Wang, Q. Gao, F. Zhu, Safety,
681 tolerability, and immunogenicity of an inactivated SARS-CoV-2 vaccine in healthy
682 adults aged 18-59 years: a randomised, double-blind, placebo-controlled, phase 1/2
683 clinical trial. *Lancet Infect Dis* **21**, 181-192 (2021).
- 684 15. N. C. Kyriakidis, A. López-Cortés, E. V. González, A. B. Grimaldos, E. O. Prado, SARS-
685 CoV-2 vaccines strategies: a comprehensive review of phase 3 candidates. *NPJ vaccines*
686 **6**, 28 (2021).
- 687 16. CTRI. Biological E's novel Covid-19 vaccine of SARS-CoV-2 for protection against
688 Covid-19 disease.,
689 <[http://ctri.nic.in/Clinicaltrials/pmaindet2.php?trialid=48329&EncHid=&userName=covi](http://ctri.nic.in/Clinicaltrials/pmaindet2.php?trialid=48329&EncHid=&userName=covid-19%20vaccine)
690 [d-19%20vaccine](http://ctri.nic.in/Clinicaltrials/pmaindet2.php?trialid=48329&EncHid=&userName=covid-19%20vaccine)> Accessed May 1, 2021
- 691 17. The New York Times. Coronavirus Vaccine Tracker,
692 <<https://www.nytimes.com/interactive/2020/science/coronavirus-vaccine-tracker.html>>,
693 Accessed May 3, 2021
- 694 18. J. Yang, W. Wang, Z. Chen, S. Lu, F. Yang, Z. Bi, L. Bao, F. Mo, X. Li, Y. Huang, W.
695 Hong, Y. Yang, Y. Zhao, F. Ye, S. Lin, W. Deng, H. Chen, H. Lei, Z. Zhang, M. Luo, H.
696 Gao, Y. Zheng, Y. Gong, X. Jiang, Y. Xu, Q. Lv, D. Li, M. Wang, F. Li, S. Wang, G.
697 Wang, P. Yu, Y. Qu, L. Yang, H. Deng, A. Tong, J. Li, Z. Wang, J. Yang, G. Shen, Z.

- 698 Zhao, Y. Li, J. Luo, H. Liu, W. Yu, M. Yang, J. Xu, J. Wang, H. Li, H. Wang, D. Kuang,
699 P. Lin, Z. Hu, W. Guo, W. Cheng, Y. He, X. Song, C. Chen, Z. Xue, S. Yao, L. Chen, X.
700 Ma, S. Chen, M. Gou, W. Huang, Y. Wang, C. Fan, Z. Tian, M. Shi, F. S. Wang, L. Dai,
701 M. Wu, G. Li, G. Wang, Y. Peng, Z. Qian, C. Huang, J. Y. Lau, Z. Yang, Y. Wei, X. Cen,
702 X. Peng, C. Qin, K. Zhang, G. Lu, X. Wei, A vaccine targeting the RBD of the S protein
703 of SARS-CoV-2 induces protective immunity. *Nature* **586**, 572-577 (2020).
- 704 19. L. Piccoli, Y. J. Park, M. A. Tortorici, N. Czudnochowski, A. C. Walls, M. Beltramello,
705 C. Silacci-Fregni, D. Pinto, L. E. Rosen, J. E. Bowen, O. J. Acton, S. Jaconi, B. Guarino,
706 A. Minola, F. Zatta, N. Sprugasci, J. Bassi, A. Peter, A. De Marco, J. C. Nix, F. Mele, S.
707 Jovic, B. F. Rodriguez, S. V. Gupta, F. Jin, G. Piumatti, G. Lo Presti, A. F. Pellanda, M.
708 Biggiogero, M. Tarkowski, M. S. Pizzuto, E. Cameroni, C. Havenar-Daughton, M.
709 Smithey, D. Hong, V. Lepori, E. Albanese, A. Ceschi, E. Bernasconi, L. Elzi, P. Ferrari,
710 C. Garzoni, A. Riva, G. Snell, F. Sallusto, K. Fink, H. W. Virgin, A. Lanzavecchia, D.
711 Corti, D. Veessler, Mapping Neutralizing and Immunodominant Sites on the SARS-CoV-
712 2 Spike Receptor-Binding Domain by Structure-Guided High-Resolution Serology. *Cell*
713 **183**, 1024-1042.e1021 (2020).
- 714 20. L. Premkumar, B. Segovia-Chumbez, R. Jadi, D. R. Martinez, R. Raut, A. Markmann, C.
715 Cornaby, L. Bartelt, S. Weiss, Y. Park, C. E. Edwards, E. Weimer, E. M. Scherer, N.
716 Rouphael, S. Edupuganti, D. Weiskopf, L. V. Tse, Y. J. Hou, D. Margolis, A. Sette, M. H.
717 Collins, J. Schmitz, R. S. Baric, A. M. de Silva, The receptor binding domain of the viral
718 spike protein is an immunodominant and highly specific target of antibodies in SARS-
719 CoV-2 patients. *Sci Immunol* **5**, (2020).

- 720 21. D. Esposito, J. Mehalko, M. Drew, K. Snead, V. Wall, T. Taylor, P. Frank, J. P. Denson,
721 M. Hong, G. Gulten, K. Sadtler, S. Messing, W. Gillette, Optimizing high-yield
722 production of SARS-CoV-2 soluble spike trimers for serology assays. *Protein Expr Purif*
723 **174**, 105686 (2020).
- 724 22. N. C. Dalvie, S. A. Rodriguez-Aponte, B. L. Hartwell, L. H. Tostanoski, A. M.
725 Biedermann, L. E. Crowell, K. Kaur, O. Kumru, L. Carter, J. Yu, A. Chang, K. McMahan,
726 T. Courant, C. Lebas, A. A. Lemnios, K. A. Rodrigues, M. Silva, R. S. Johnston, C. A.
727 Naranjo, M. K. Tracey, J. R. Brady, C. A. Whittaker, D. Yun, S. Kar, M. Porto, M. Lok,
728 H. Andersen, M. G. Lewis, K. R. Love, D. L. Camp, J. M. Silverman, H. Kleanthous, S.
729 B. Joshi, D. B. Volkin, P. M. Dubois, N. Collin, N. P. King, D. H. Barouch, D. J. Irvine, J.
730 C. Love, Engineered SARS-CoV-2 receptor binding domain improves immunogenicity in
731 mice and elicits protective immunity in hamsters. *bioRxiv*, (2021).
- 732 23. S. Yang, Y. Li, L. Dai, J. Wang, P. He, C. Li, X. Fang, C. Wang, X. Zhao, E. Huang, C.
733 Wu, Z. Zhong, F. Wang, X. Duan, S. Tian, L. Wu, Y. Liu, Y. Luo, Z. Chen, F. Li, J. Li,
734 X. Yu, H. Ren, L. Liu, S. Meng, J. Yan, Z. Hu, L. Gao, G. F. Gao, Safety and
735 immunogenicity of a recombinant tandem-repeat dimeric RBD-based protein subunit
736 vaccine (ZF2001) against COVID-19 in adults: two randomised, double-blind, placebo-
737 controlled, phase 1 and 2 trials. *Lancet Infect Dis*, (2021).
- 738 24. L. Dai, T. Zheng, K. Xu, Y. Han, L. Xu, E. Huang, Y. An, Y. Cheng, S. Li, M. Liu, M.
739 Yang, Y. Li, H. Cheng, Y. Yuan, W. Zhang, C. Ke, G. Wong, J. Qi, C. Qin, J. Yan, G. F.
740 Gao, A Universal Design of Betacoronavirus Vaccines against COVID-19, MERS, and
741 SARS. *Cell* **182**, 722-733.e711 (2020).

- 742 25. B. M. Hauser, M. Sangesland, E. C. Lam, J. Feldman, A. S. Yousif, T. M. Caradonna, A.
743 B. Balazs, D. Lingwood, A. G. Schmidt, Engineered receptor binding domain
744 immunogens elicit pan-coronavirus neutralizing antibodies. *bioRxiv*, (2020).
- 745 26. T. K. Tan, P. Rijal, R. Rahikainen, A. H. Keeble, L. Schimanski, S. Hussain, R. Harvey, J.
746 W. P. Hayes, J. C. Edwards, R. K. McLean, V. Martini, M. Pedrera, N. Thakur, C.
747 Conceicao, I. Dietrich, H. Shelton, A. Ludi, G. Wilsden, C. Browning, A. K. Zagrajek, D.
748 Bialy, S. Bhat, P. Stevenson-Leggett, P. Hollinghurst, M. Tully, K. Moffat, C. Chiu, R.
749 Waters, A. Gray, M. Azhar, V. Mioulet, J. Newman, A. S. Asfor, A. Burman, S. Crossley,
750 J. A. Hammond, E. Tchilian, B. Charleston, D. Bailey, T. J. Tuthill, S. P. Graham, H. M.
751 E. Duyvesteyn, T. Malinauskas, J. Huo, J. A. Tree, K. R. Buttigieg, R. J. Owens, M. W.
752 Carroll, R. S. Daniels, J. W. McCauley, D. I. Stuart, K. A. Huang, M. Howarth, A. R.
753 Townsend, A COVID-19 vaccine candidate using SpyCatcher multimerization of the
754 SARS-CoV-2 spike protein receptor-binding domain induces potent neutralising antibody
755 responses. *Nature communications* **12**, 542 (2021).
- 756 27. A. C. Walls, B. Fiala, A. Schäfer, S. Wrenn, M. N. Pham, M. Murphy, L. V. Tse, L.
757 Shehata, M. A. O'Connor, C. Chen, M. J. Navarro, M. C. Miranda, D. Pettie, R.
758 Ravichandran, J. C. Kraft, C. Ogohara, A. Palser, S. Chalk, E. C. Lee, K. Guerriero, E.
759 Kepl, C. M. Chow, C. Sydeman, E. A. Hodge, B. Brown, J. T. Fuller, K. H. Dinnon, 3rd,
760 L. E. Gralinski, S. R. Leist, K. L. Gully, T. B. Lewis, M. Guttman, H. Y. Chu, K. K. Lee,
761 D. H. Fuller, R. S. Baric, P. Kellam, L. Carter, M. Pepper, T. P. Sheahan, D. Veessler, N.
762 P. King, Elicitation of Potent Neutralizing Antibody Responses by Designed Protein
763 Nanoparticle Vaccines for SARS-CoV-2. *Cell* **183**, 1367-1382.e1317 (2020).

- 764 28. L. Yang, D. Tian, J.-b. Han, W. Fan, Y. Zhang, Y. Li, W. Sun, Y. Wei, X. Tian, D.-d. Yu,
765 X.-l. Feng, G. Cheng, Y.-t. Zheng, Y. Bi, W. Liu, A recombinant receptor-binding
766 domain in trimeric form generates completely protective immunity against SARS-CoV-2
767 infection in nonhuman primates. *bioRxiv*, 2021.2003.2030.437647 (2021).
- 768 29. L. He, X. Lin, Y. Wang, C. Abraham, C. Sou, T. Ngo, Y. Zhang, I. A. Wilson, J. Zhu,
769 Single-component, self-assembling, protein nanoparticles presenting the receptor binding
770 domain and stabilized spike as SARS-CoV-2 vaccine candidates. *Sci Adv* **7**, (2021).
- 771 30. S. G. Reed, M. Tomai, M. J. Gale, Jr., New horizons in adjuvants for vaccine
772 development. *Curr Opin Immunol* **65**, 97-101 (2020).
- 773 31. B. Pulendran, S. A. P, D. T. O'Hagan, Emerging concepts in the science of vaccine
774 adjuvants. *Nature reviews. Drug discovery*, 1-22 (2021).
- 775 32. D. T. O'Hagan, R. N. Lodaya, G. Lofano, The continued advance of vaccine adjuvants -
776 'we can work it out'. *Seminars in immunology* **50**, 101426 (2020).
- 777 33. H. Lal, A. L. Cunningham, O. Godeaux, R. Chlibek, J. Díez-Domingo, S. J. Hwang, M. J.
778 Levin, J. E. McElhaney, A. Poder, J. Puig-Barberà, T. Vesikari, D. Watanabe, L. Weckx,
779 T. Zahaf, T. C. Heineman, Efficacy of an adjuvanted herpes zoster subunit vaccine in
780 older adults. *The New England journal of medicine* **372**, 2087-2096 (2015).
- 781 34. A. L. Cunningham, H. Lal, M. Kovac, R. Chlibek, S. J. Hwang, J. Díez-Domingo, O.
782 Godeaux, M. J. Levin, J. E. McElhaney, J. Puig-Barberà, C. Vanden Abeele, T. Vesikari,
783 D. Watanabe, T. Zahaf, A. Ahonen, E. Athan, J. F. Barba-Gomez, L. Campora, F. de
784 Looze, H. J. Downey, W. Ghesquiere, I. Gorfinkel, T. Korhonen, E. Leung, S. A. McNeil,
785 L. Oostvogels, L. Rombo, J. Smetana, L. Weckx, W. Yeo, T. C. Heineman, Efficacy of

- 786 the Herpes Zoster Subunit Vaccine in Adults 70 Years of Age or Older. *The New*
787 *England journal of medicine* **375**, 1019-1032 (2016).
- 788 35. S. R. Leist, K. H. Dinnon, 3rd, A. Schäfer, L. V. Tse, K. Okuda, Y. J. Hou, A. West, C. E.
789 Edwards, W. Sanders, E. J. Fritch, K. L. Gully, T. Scobey, A. J. Brown, T. P. Sheahan, N.
790 J. Moorman, R. C. Boucher, L. E. Gralinski, S. A. Montgomery, R. S. Baric, A Mouse-
791 Adapted SARS-CoV-2 Induces Acute Lung Injury and Mortality in Standard Laboratory
792 Mice. *Cell* **183**, 1070-1085.e1012 (2020).
- 793 36. K. Lederer, D. Castaño, D. Gómez Atria, T. H. Oguin, 3rd, S. Wang, T. B. Manzoni, H.
794 Muramatsu, M. J. Hogan, F. Amanat, P. Cherubin, K. A. Lundgreen, Y. K. Tam, S. H. Y.
795 Fan, L. C. Eisenlohr, I. Maillard, D. Weissman, P. Bates, F. Krammer, G. D. Sempowski,
796 N. Pardi, M. Locci, SARS-CoV-2 mRNA Vaccines Foster Potent Antigen-Specific
797 Germinal Center Responses Associated with Neutralizing Antibody Generation.
798 *Immunity* **53**, 1281-1295.e1285 (2020).
- 799 37. J. G. Liang, D. Su, T. Z. Song, Y. Zeng, W. Huang, J. Wu, R. Xu, P. Luo, X. Yang, X.
800 Zhang, S. Luo, Y. Liang, X. Li, J. Huang, Q. Wang, X. Huang, Q. Xu, M. Luo, A. Huang,
801 D. Luo, C. Zhao, F. Yang, J. B. Han, Y. T. Zheng, P. Liang, S-Trimer, a COVID-19
802 subunit vaccine candidate, induces protective immunity in nonhuman primates. *Nature*
803 *communications* **12**, 1346 (2021).
- 804 38. W. F. Garcia-Beltran, E. C. Lam, K. St Denis, A. D. Nitido, Z. H. Garcia, B. M. Hauser, J.
805 Feldman, M. N. Pavlovic, D. J. Gregory, M. C. Poznansky, A. Sigal, A. G. Schmidt, A. J.
806 Iafate, V. Naranbhai, A. B. Balazs, Multiple SARS-CoV-2 variants escape neutralization
807 by vaccine-induced humoral immunity. *Cell*, (2021).

- 808 39. A. Kuzmina, Y. Khalaila, O. Voloshin, A. Keren-Naus, L. Boehm-Cohen, Y. Raviv, Y.
809 Shemer-Avni, E. Rosenberg, R. Taube, SARS-CoV-2 spike variants exhibit differential
810 infectivity and neutralization resistance to convalescent or post-vaccination sera. *Cell*
811 *host & microbe*, (2021).
- 812 40. X. Shen, H. Tang, R. Pajon, G. Smith, G. M. Glenn, W. Shi, B. Korber, D. C. Montefiori,
813 Neutralization of SARS-CoV-2 Variants B.1.429 and B.1.351. *The New England journal*
814 *of medicine*, (2021).
- 815 41. Z. Wang, F. Schmidt, Y. Weisblum, F. Muecksch, C. O. Barnes, S. Finkin, D. Schaefer-
816 Babajew, M. Cipolla, C. Gaebler, J. A. Lieberman, T. Y. Oliveira, Z. Yang, M. E.
817 Abernathy, K. E. Huey-Tubman, A. Hurley, M. Turroja, K. A. West, K. Gordon, K. G.
818 Millard, V. Ramos, J. Da Silva, J. Xu, R. A. Colbert, R. Patel, J. Dizon, C. Unson-
819 O'Brien, I. Shimeliovich, A. Gazumyan, M. Caskey, P. J. Bjorkman, R. Casellas, T.
820 Hatzioannou, P. D. Bieniasz, M. C. Nussenzweig, mRNA vaccine-elicited antibodies to
821 SARS-CoV-2 and circulating variants. *Nature* **592**, 616-622 (2021).
- 822 42. L. J. Abu-Raddad, H. Chemaitelly, A. A. Butt, Effectiveness of the BNT162b2 Covid-19
823 Vaccine against the B.1.1.7 and B.1.351 Variants. *The New England journal of medicine*,
824 (2021).
- 825 43. A. Iwasaki, R. Medzhitov, Control of adaptive immunity by the innate immune system.
826 *Nat Immunol* **16**, 343-353 (2015).
- 827 44. A. J. Pollard, E. M. Bijker, A guide to vaccinology: from basic principles to new
828 developments. *Nature reviews. Immunology* **21**, 83-100 (2021).
- 829 45. S. M. Grant, M. Lou, L. Yao, R. N. Germain, A. J. Radtke, The lymph node at a glance -
830 how spatial organization optimizes the immune response. *J Cell Sci* **133**, (2020).

- 831 46. S. E. Acton, C. Reis e Sousa, Dendritic cells in remodeling of lymph nodes during
832 immune responses. *Immunol Rev* **271**, 221-229 (2016).
- 833 47. E. J. Williamson, A. J. Walker, K. Bhaskaran, S. Bacon, C. Bates, C. E. Morton, H. J.
834 Curtis, A. Mehrkar, D. Evans, P. Inglesby, J. Cockburn, H. I. McDonald, B. MacKenna,
835 L. Tomlinson, I. J. Douglas, C. T. Rentsch, R. Mathur, A. Y. S. Wong, R. Grieve, D.
836 Harrison, H. Forbes, A. Schultze, R. Croker, J. Parry, F. Hester, S. Harper, R. Perera, S. J.
837 W. Evans, L. Smeeth, B. Goldacre, Factors associated with COVID-19-related death
838 using OpenSAFELY. *Nature* **584**, 430-436 (2020).
- 839 48. Centers for Disease Control and Prevention (CDC). COVID-19 Hospitalization and
840 Death by Age, Accessed Apr 3rd, 2021, 2021
- 841 49. P. J. Hotez, M. E. Bottazzi, Developing a low-cost and accessible COVID-19 vaccine for
842 global health. *PLoS Negl Trop Dis* **14**, e0008548 (2020).
- 843 50. K. McMahan, J. Yu, N. B. Mercado, C. Loos, L. H. Tostanoski, A. Chandrashekar, J. Liu,
844 L. Peter, C. Atyeo, A. Zhu, E. A. Bondzie, G. Dagotto, M. S. Gebre, C. Jacob-Dolan, Z.
845 Li, F. Nampanya, S. Patel, L. Pessaint, A. Van Ry, K. Blade, J. Yalley-Ogunro, M. Cabus,
846 R. Brown, A. Cook, E. Teow, H. Andersen, M. G. Lewis, D. A. Lauffenburger, G. Alter,
847 D. H. Barouch, Correlates of protection against SARS-CoV-2 in rhesus macaques.
848 *Nature*, (2020).
- 849 51. P. S. Arunachalam, A. C. Walls, N. Golden, C. Atyeo, S. Fischinger, C. Li, P. Aye, M. J.
850 Navarro, L. Lai, V. V. Edara, K. Röltgen, K. Rogers, L. Shirreff, D. E. Ferrell, S. Wrenn,
851 D. Pettie, J. C. Kraft, M. C. Miranda, E. Kepl, C. Sydeman, N. Brunette, M. Murphy, B.
852 Fiala, L. Carter, A. G. White, M. Trisal, C.-L. Hsieh, K. Russell-Lodrigue, C. Monjure, J.
853 Dufour, L. Doyle-Meyer, R. B. Bohm, N. J. Maness, C. Roy, J. A. Plante, K. S. Plante, A.

- 854 Zhu, M. J. Gorman, S. Shin, X. Shen, J. Fontenot, S. Gupta, D. T. O'Hagan, R. V. D.
855 Most, R. Rappuoli, R. L. Coffman, D. Novack, J. S. McLellan, S. Subramaniam, D.
856 Montefiori, S. D. Boyd, J. L. Flynn, G. Alter, F. Villinger, H. Kleanthous, J. Rappaport,
857 M. Suthar, N. P. King, D. Veessler, B. Pulendran, Adjuvanting a subunit SARS-CoV-2
858 nanoparticle vaccine to induce protective immunity in non-human primates. *bioRxiv*,
859 2021.2002.2010.430696 (2021).
- 860 52. W. H. Chen, J. Wei, R. T. Kundu, R. Adhikari, Z. Liu, J. Lee, L. Versteeg, C. Poveda, B.
861 Keegan, M. J. Villar, A. C. de Araujo Leao, J. A. Rivera, P. M. Gillespie, J. Pollet, U.
862 Strych, B. Zhan, P. J. Hotez, M. E. Bottazzi, Genetic modification to design a stable
863 yeast-expressed recombinant SARS-CoV-2 receptor binding domain as a COVID-19
864 vaccine candidate. *Biochim Biophys Acta Gen Subj* **1865**, 129893 (2021).
- 865 53. W. H. Chen, X. Tao, A. S. Agrawal, A. Algaissi, B. H. Peng, J. Pollet, U. Strych, M. E.
866 Bottazzi, P. J. Hotez, S. Lustigman, L. Du, S. Jiang, C. K. Tseng, Yeast-expressed SARS-
867 CoV recombinant receptor-binding domain (RBD219-N1) formulated with aluminum
868 hydroxide induces protective immunity and reduces immune enhancement. *Vaccine* **38**,
869 7533-7541 (2020).
- 870 54. J. Pollet, W. H. Chen, L. Versteeg, B. Keegan, B. Zhan, J. Wei, Z. Liu, J. Lee, R. Kundu,
871 R. Adhikari, C. Poveda, M. J. Villar, A. C. de Araujo Leao, J. Altieri Rivera, Z. Momin,
872 P. M. Gillespie, J. T. Kimata, U. Strych, P. J. Hotez, M. E. Bottazzi, SARS-CoV-2
873 RBD219-N1C1: A yeast-expressed SARS-CoV-2 recombinant receptor-binding domain
874 candidate vaccine stimulates virus neutralizing antibodies and T-cell immunity in mice.
875 *Human vaccines & immunotherapeutics*, 1-11 (2021).

- 876 55. J. Paavonen, P. Naud, J. Salmerón, C. M. Wheeler, S. N. Chow, D. Apter, H. Kitchener,
877 X. Castellsague, J. C. Teixeira, S. R. Skinner, J. Hedrick, U. Jaisamrarn, G. Limson, S.
878 Garland, A. Szarewski, B. Romanowski, F. Y. Aoki, T. F. Schwarz, W. A. Poppe, F. X.
879 Bosch, D. Jenkins, K. Hardt, T. Zahaf, D. Descamps, F. Struyf, M. Lehtinen, G. Dubin,
880 Efficacy of human papillomavirus (HPV)-16/18 AS04-adjuvanted vaccine against
881 cervical infection and precancer caused by oncogenic HPV types (PATRICIA): final
882 analysis of a double-blind, randomised study in young women. *Lancet (London, England)*
883 **374**, 301-314 (2009).
- 884 56. J. D. Campbell, Development of the CpG Adjuvant 1018: A Case Study. *Methods in*
885 *molecular biology (Clifton, N.J.)* **1494**, 15-27 (2017).
- 886 57. C. L. Cooper, H. L. Davis, M. L. Morris, S. M. Efler, M. A. Adhami, A. M. Krieg, D. W.
887 Cameron, J. Heathcote, CPG 7909, an immunostimulatory TLR9 agonist
888 oligodeoxynucleotide, as adjuvant to Engerix-B HBV vaccine in healthy adults: a double-
889 blind phase I/II study. *J Clin Immunol* **24**, 693-701 (2004).
- 890 58. B. Maletto, A. Rópolo, V. Morón, M. C. Pistoiresi-Palencia, CpG-DNA stimulates
891 cellular and humoral immunity and promotes Th1 differentiation in aged BALB/c mice.
892 *Journal of leukocyte biology* **72**, 447-454 (2002).
- 893 59. B. A. Maletto, A. S. Rópolo, M. V. Liscovsky, D. O. Alignani, M. Glocker, M. C.
894 Pistoiresi-Palencia, CpG oligodeoxynucleotides functions as an effective adjuvant in aged
895 BALB/c mice. *Clinical immunology (Orlando, Fla.)* **117**, 251-261 (2005).
- 896 60. B. M. Manning, E. Y. Enioutina, D. M. Visic, A. D. Knudson, R. A. Daynes, CpG DNA
897 functions as an effective adjuvant for the induction of immune responses in aged mice.
898 *Exp Gerontol* **37**, 107-126 (2001).

- 899 61. F. Ming, J. Yang, P. Chu, M. Ma, J. Shi, H. Cai, C. Huang, H. Li, Z. Jiang, H. Wang, W.
900 Wang, S. Zhang, L. Zhang, Immunization of aged pigs with attenuated pseudorabies
901 virus vaccine combined with CpG oligodeoxynucleotide restores defective Th1 immune
902 responses. *PloS one* **8**, e65536 (2013).
- 903 62. W. Qin, J. Jiang, Q. Chen, N. Yang, Y. Wang, X. Wei, R. Ou, CpG ODN enhances
904 immunization effects of hepatitis B vaccine in aged mice. *Cell Mol Immunol* **1**, 148-152
905 (2004).
- 906 63. G. Sen, Q. Chen, C. M. Snapper, Immunization of aged mice with a pneumococcal
907 conjugate vaccine combined with an unmethylated CpG-containing oligodeoxynucleotide
908 restores defective immunoglobulin G antipolysaccharide responses and specific CD4+-T-
909 cell priming to young adult levels. *Infection and immunity* **74**, 2177-2186 (2006).
- 910 64. B. P. Sablan, D. J. Kim, N. G. Barzaga, W. C. Chow, M. Cho, S. H. Ahn, S. G. Hwang, J.
911 H. Lee, H. Namini, W. L. Heyward, Demonstration of safety and enhanced
912 seroprotection against hepatitis B with investigational HBsAg-1018 ISS vaccine
913 compared to a licensed hepatitis B vaccine. *Vaccine* **30**, 2689-2696 (2012).
- 914 65. J. M. Janssen, S. Jackson, W. L. Heyward, R. S. Janssen, Immunogenicity of an
915 investigational hepatitis B vaccine with a toll-like receptor 9 agonist adjuvant (HBsAg-
916 1018) compared with a licensed hepatitis B vaccine in subpopulations of healthy adults
917 18-70 years of age. *Vaccine* **33**, 3614-3618 (2015).
- 918 66. T. Y. Kuo, M. Y. Lin, R. L. Coffman, J. D. Campbell, P. Traquina, Y. J. Lin, L. T. Liu, J.
919 Cheng, Y. C. Wu, C. C. Wu, W. H. Tang, C. G. Huang, K. C. Tsao, C. Chen,
920 Development of CpG-adjuvanted stable prefusion SARS-CoV-2 spike antigen as a
921 subunit vaccine against COVID-19. *Sci Rep* **10**, 20085 (2020).

- 922 67. C.-E. Lien, Y.-J. Lin, C. Chen, W.-C. Lian, T.-Y. Kuo, J. D. Campbell, P. Traquina, M.-
923 Y. Lin, L. T.-C. Liu, Y.-S. Chuang, H.-Y. Ko, C.-C. Liao, Y.-H. Chen, J.-T. Jan, C.-P.
924 Sun, Y.-S. Lin, P.-Y. Wu, Y.-C. Wang, M.-H. Tao, Y.-L. Lin, CpG-adjuvanted stable
925 prefusion SARS-CoV-2 spike protein protected hamsters from SARS-CoV-2 challenge.
926 *bioRxiv*, 2021.2001.2007.425674 (2021).
- 927 68. N. Kayraklioglu, B. Horuluoglu, D. M. Klinman, CpG Oligonucleotides as Vaccine
928 Adjuvants. *Methods in molecular biology (Clifton, N.J.)* **2197**, 51-85 (2021).
- 929 69. D. J. Dowling, S. D. van Haren, A. Scheid, I. Bergelson, D. Kim, C. J. Mancuso, W.
930 Foppen, A. Ozonoff, L. Fresh, T. B. Theriot, A. A. Lackner, R. N. Fichorova, D. Smirnov,
931 J. P. Vasilakos, J. M. Beaurline, M. A. Tomai, C. C. Midkiff, X. Alvarez, J. L. Blanchard,
932 M. H. Gilbert, P. P. Aye, O. Levy, TLR7/8 adjuvant overcomes newborn
933 hyporesponsiveness to pneumococcal conjugate vaccine at birth. *JCI insight* **2**, e91020
934 (2017).
- 935 70. C. Garrido, A. D. Curtis, M. Dennis, S. H. Pathak, H. Gao, D. Montefiori, M. Tomai, C.
936 B. Fox, P. A. Kozlowski, T. Scobey, J. E. Munt, M. L. Mallroy, P. T. Saha, M. G.
937 Hudgens, L. C. Lindesmith, R. S. Baric, O. M. Abiona, B. Graham, K. S. Corbett, D.
938 Edwards, A. Carfi, G. Fouda, K. K. A. Van Rompay, K. De Paris, S. R. Permar, SARS-
939 CoV-2 Vaccines Elicit Durable Immune Responses in Infant Rhesus Macaques. *bioRxiv*,
940 2021.2004.2005.438479 (2021).
- 941 71. K. Wu, A. Choi, M. Koch, S. Elbashir, L. Ma, D. Lee, A. Woods, C. Henry, C.
942 Palandjian, A. Hill, J. Quinones, N. Nunna, S. O'Connell, A. B. McDermott, S. Falcone,
943 E. Narayanan, T. Colpitts, H. Bennett, K. Corbett, R. Seder, B. S. Graham, G. B. Stewart-
944 Jones, A. Carfi, D. K. Edwards, Variant SARS-CoV-2 mRNA vaccines confer broad

- 945 neutralization as primary or booster series in mice. *bioRxiv*, 2021.2004.2013.439482
946 (2021).
- 947 72. N. W. Baylor, W. Egan, P. Richman, Aluminum salts in vaccines--US perspective.
948 *Vaccine* **20 Suppl 3**, S18-23 (2002).
- 949 73. F. Borriello, C. Pietrasanta, J. C. Y. Lai, L. M. Walsh, P. Sharma, D. N. O'Driscoll, J.
950 Ramirez, S. Brightman, L. Pagni, F. Mosca, D. J. Burkhart, D. J. Dowling, O. Levy,
951 Identification and Characterization of Stimulator of Interferon Genes As a Robust
952 Adjuvant Target for Early Life Immunization. *Front Immunol* **8**, 1772 (2017).
- 953 74. C. W. Tan, W. N. Chia, X. Qin, P. Liu, M. I. Chen, C. Tiu, Z. Hu, V. C. Chen, B. E.
954 Young, W. R. Sia, Y. J. Tan, R. Foo, Y. Yi, D. C. Lye, D. E. Anderson, L. F. Wang, A
955 SARS-CoV-2 surrogate virus neutralization test based on antibody-mediated blockage of
956 ACE2-spike protein-protein interaction. *Nat Biotechnol* **38**, 1073-1078 (2020).
- 957 75. J. Yu, L. H. Tostanoski, L. Peter, N. B. Mercado, K. McMahan, S. H. Mahrokhian, J. P.
958 Nkolola, J. Liu, Z. Li, A. Chandrashekar, D. R. Martinez, C. Loos, C. Atyeo, S.
959 Fischinger, J. S. Burke, M. D. Slein, Y. Chen, A. Zuiani, F. J. N. Lelis, M. Travers, S.
960 Habibi, L. Pessaint, A. Van Ry, K. Blade, R. Brown, A. Cook, B. Finneyfrock, A.
961 Dodson, E. Teow, J. Velasco, R. Zahn, F. Wegmann, E. A. Bondzie, G. Dagotto, M. S.
962 Gebre, X. He, C. Jacob-Dolan, M. Kirilova, N. Kordana, Z. Lin, L. F. Maxfield, F.
963 Nampanya, R. Nityanandam, J. D. Ventura, H. Wan, Y. Cai, B. Chen, A. G. Schmidt, D.
964 R. Wesemann, R. S. Baric, G. Alter, H. Andersen, M. G. Lewis, D. H. Barouch, DNA
965 vaccine protection against SARS-CoV-2 in rhesus macaques. *Science* **369**, 806-811
966 (2020).

- 967 76. J. Yu, Z. Li, X. He, M. S. Gebre, E. A. Bondzie, H. Wan, C. Jacob-Dolan, D. R. Martinez,
968 J. P. Nkolola, R. S. Baric, D. H. Barouch, Deletion of the SARS-CoV-2 Spike
969 Cytoplasmic Tail Increases Infectivity in Pseudovirus Neutralization Assays. *Journal of*
970 *Virology*, JVI.00044-00021 (2021).
- 971 77. S. D. van Haren, D. J. Dowling, W. Foppen, D. Christensen, P. Andersen, S. G. Reed, R.
972 M. Hershberg, L. R. Baden, O. Levy, Age-Specific Adjuvant Synergy: Dual TLR7/8 and
973 Mincle Activation of Human Newborn Dendritic Cells Enables Th1 Polarization. *Journal*
974 *of immunology (Baltimore, Md. : 1950)* **197**, 4413-4424 (2016).
- 975 78. M. C. Berenbaum, Correlations between methods for measurement of synergy. *The*
976 *Journal of infectious diseases* **142**, 476-480 (1980).
- 977

978 **ACKNOWLEDGEMENTS**

979 We thank the members of the BCH *Precision Vaccine Program* for helpful discussions. We
980 thank Drs. Kevin Churchwell, Gary Fleisher, David Williams, and Mr. August Cervini for their
981 support of the *Precision Vaccines Program*. We thank Dr. Barney S. Graham (NIH Vaccine
982 Research Center) for generously providing the plasmid for pre-fusion stabilized SARS-CoV-2
983 Spike trimer. We thank Dr. Ralph Baric for providing the SARS-CoV-2/MA10 virus. We thank
984 the pharmacists of Boston Children's Hospital for their efforts to maximize the use of SARS-
985 CoV-2 vaccines by saving leftover or overfill of otherwise to be discarded vaccine vials. D.J.D.
986 would like to thank Ms. Siobhan McHugh, Ms. Geneva Boyer, Mrs. Lucy Conetta and the staff
987 of Lucy's Daycare, the staff the YMCA of Greater Boston, Bridging Independent Living
988 Together (BILT), Inc., and the Boston Public Schools for childcare and educational support
989 during the COVID-19 pandemic.

990

991 **FUNDING**

992 The current study was supported in part by US National Institutes of Health (NIH)/National
993 Institutes of Allergy and Infectious Diseases (NIAID) awards, including Adjuvant Discovery
994 (HHSN272201400052C and 75N93019C00044) and Development (HHSN272201800047C)
995 Program Contracts to O.L. D.J.D.'s laboratory is supported by NIH grant (1R21AI137932-01A1),
996 Adjuvant Discovery Program contract (75N93019C00044). R.E.H. is supported by the U.S.
997 Army's Long Term Health and Education Training Program and M.B.F. is partially supported by
998 BARDA# ASPR-20-01495, DARPA# ASPR-20-01495, NIH R01 AI148166, and NIH
999 HHSN272201400007C. A.G.S.'s laboratory is supported by NIH R01 AI146779 (A.G.S.),
1000 NIGMS T32 GM007753 (B.M.H. and T.M.C.), T32 AI007245 (J.F.), and a Massachusetts

1001 Consortium on Pathogenesis Readiness (MassCPR) grant to A.G.S. I.Z. is supported by NIH
1002 grants 1R01AI121066 and 1R01DK115217, and holds an Investigators in the Pathogenesis of
1003 Infectious Disease Award from the Burroughs Wellcome Fund. The *Precision Vaccines Program*
1004 is supported in part by the BCH Department of Pediatrics and the Chief Scientific Office. E.N. is
1005 supported by the Daiichi Sankyo Foundation of Life Science and Uehara Memorial Foundation
1006 and is a joint Society for Pediatric Research and Japanese Pediatric Society Scholar.

1007

1008 **AUTHOR CONTRIBUTIONS**

1009 EN and FB conceived, designed, performed, analyzed the experiments and wrote the paper; TRO,
1010 YS, BB, MDL, KC, MMe, SDG, and SVH performed *in vitro* and/or *in vivo* experiments and
1011 their analysis; JC and JD-A performed the analysis of the qPCR data; KS, AZX, HSS, SDP,
1012 TMC, JF, BMH, AGS expressed and purified SARS-CoV-2 RBD and Spike; MEM, REH, CD,
1013 SMW, RMJ, HLH, RM, AB and MBF performed and analyzed SARS-CoV-2 neutralization
1014 experiments and mouse challenge study; AC, JY and DHB performed and analyzed pseudovirus
1015 neutralization experiments; ACS and LRB contributed to the human elderly *in vitro* analysis;
1016 MEB, PJH, and US edited and critically reviewed the manuscript; RKE and IZ contributed to the
1017 design of experiments; AO provided design feedback and contributed to the statistical analysis;
1018 OL and DJD conceived the project, designed the experiments, supervised the study and wrote the
1019 paper.

1020

1021 **COMPETING INTERESTS STATEMENT**

1022 EN, FB, TRO, YS, SVH, OL, and DJD are named inventors on vaccine adjuvant patents
1023 assigned to Boston Children's Hospital. FB has signed consulting agreements with Merck

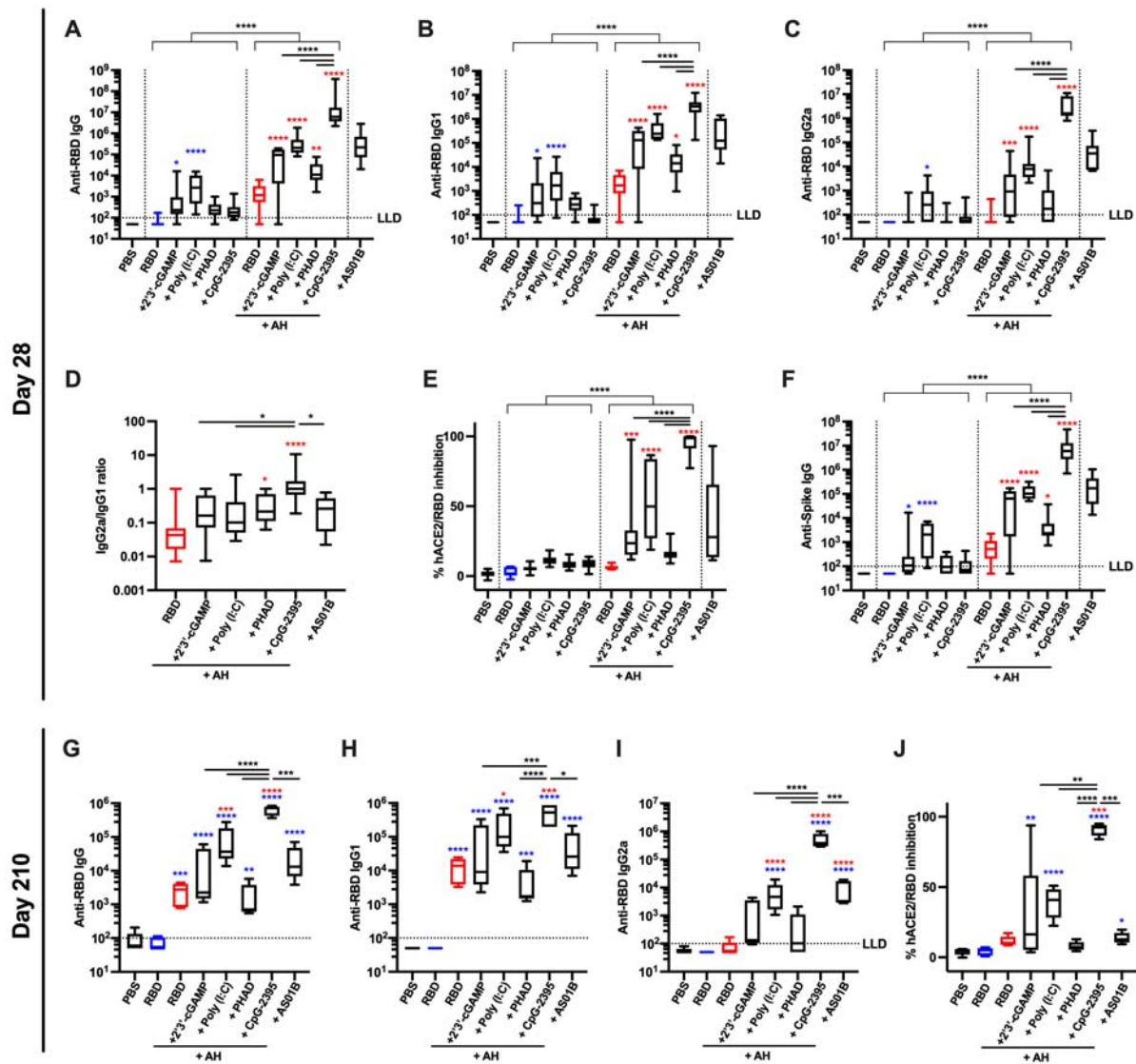
1024 Sharp & Dohme Corp. (a subsidiary of Merck & Co., Inc.), Sana Biotechnology, Inc., and F.
1025 Hoffmann-La Roche Ltd. IZ reports compensation for consulting services with Implicit
1026 Biosciences. MF is on the advisory board of Aikido Pharma. The BCM authors declare they are
1027 developers of a recombinant RBD technology. Baylor College of Medicine recently licensed the
1028 technology to Biological E, an Indian manufacturer, for advancement and licensure.
1029 These commercial or financial relationships are unrelated to the current study.

1030

1031 **DATA AND MATERIALS AVAILABILITY**

1032 All data are available in the main text or the supplementary materials

1033



1034

1035 **Figure 1. RBD formulated with AH:CpG induces robust production of anti-RBD**

1036 **neutralizing antibodies in young adult mice**

1037 Young adult, 3-month-old BALB/c mice were immunized IM on Days 0 and 14 with 10 μ g of

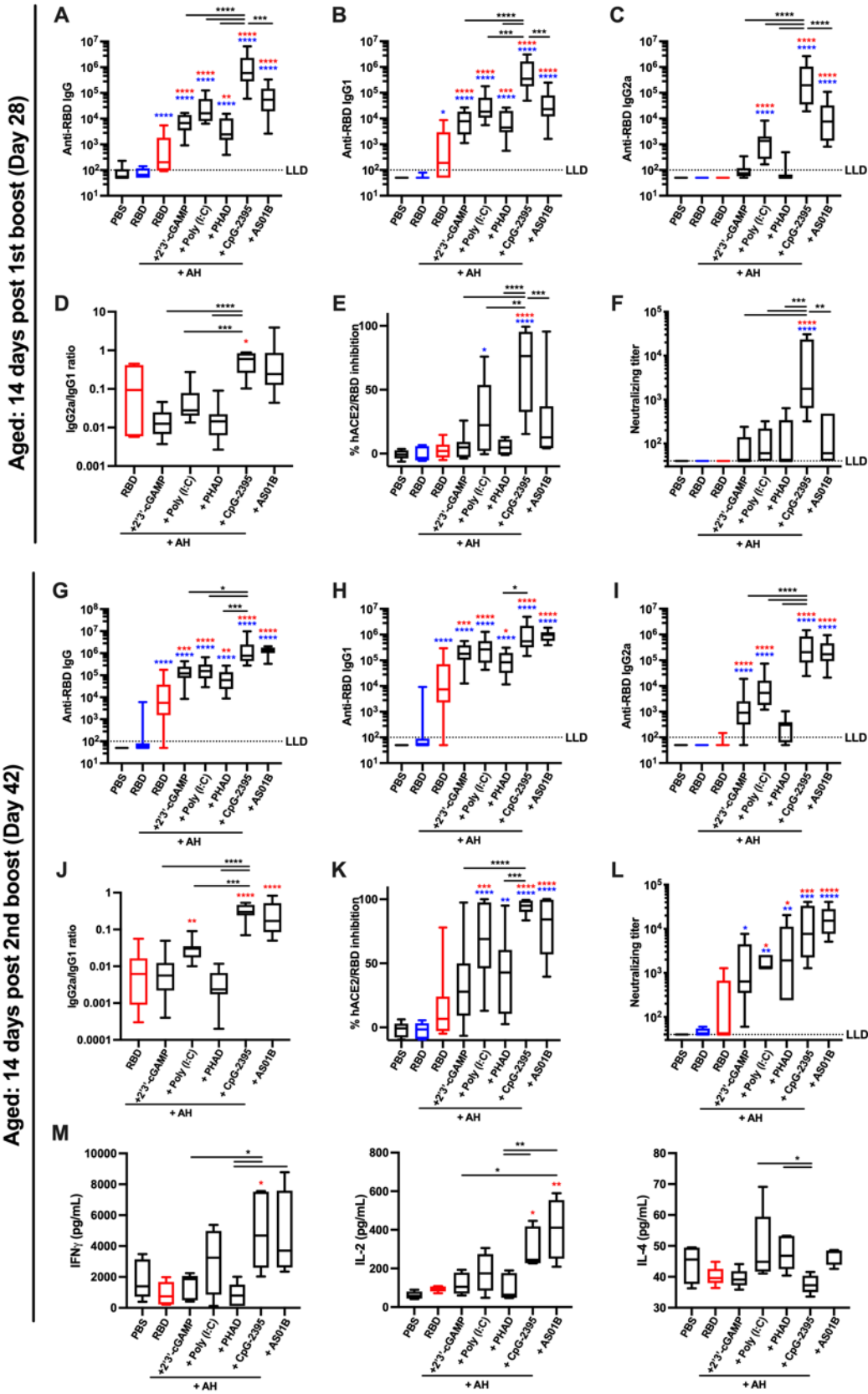
1038 monomeric SARS-CoV-2 RBD protein with indicated adjuvants. Each PRR agonist was

1039 administered alone or formulated with aluminum hydroxide (AH). (A–F) Serum samples were

1040 collected on Day 28, and (A) Anti-RBD IgG, (B) IgG1, (C) IgG2a, (D) IgG2a/IgG1 ratio,

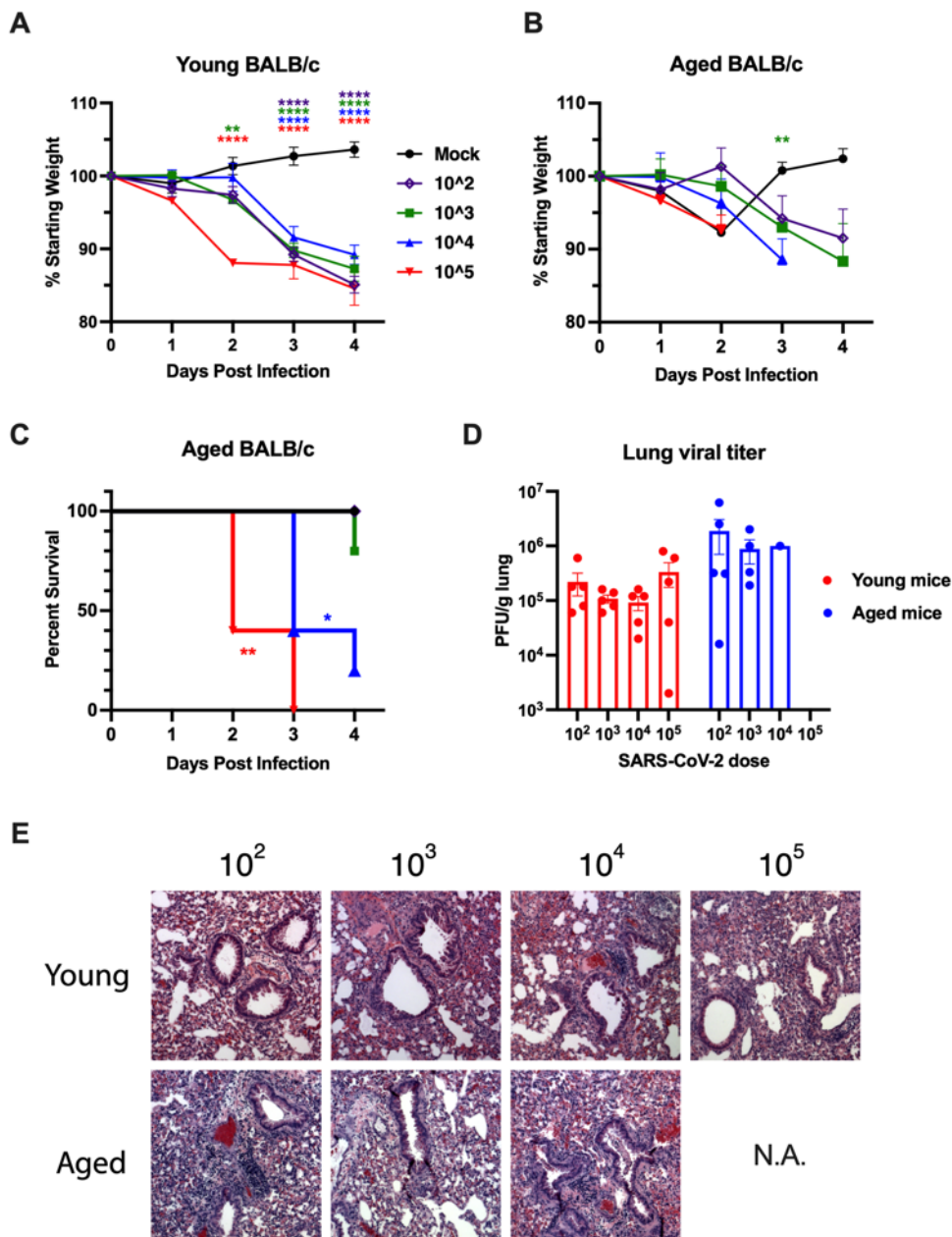
1041 hACE2/RBD inhibition rate, and (F) anti-Spike IgG were assessed. N=10 per group. Data were

1042 combined from two individual experiments. **(G–J)** Serum samples were collected on Day 210,
1043 and **(G)** Anti-RBD IgG, **(H)** IgG1, **(I)** IgG2a and **(J)** hACE2/RBD inhibition rate were assessed.
1044 N=5 per group. Data were analyzed by two-way **(A–C, E–F)** (AH and PRR agonist) or one-way
1045 **(D, G–J)** ANOVAs followed by post-hoc Tukey's test for multiple comparisons. * $P < 0.05$, ** P
1046 < 0.01 , *** $P < 0.001$, **** $P < 0.0001$. Blue and red colored asterisks respectively indicate
1047 comparisons to RBD and AH adjuvanted RBD groups. Box-and-whisker plots represent the
1048 minimum, first quartile, median, third quartile, and maximum value. LLD, lower limit of
1049 detection.



1050

1051 **Figure 2. AH:CpG adjuvant formulation elicits a robust anti-RBD response in aged mice**
1052 Aged, 14-month-old BALB/c mice were immunized IM on Days 0, 14, and 28 with 10 µg of
1053 monomeric SARS-CoV-2 RBD protein with indicated adjuvants. Each PRR agonist was
1054 formulated with aluminum hydroxide (AH). Serum samples were collected and analyzed on day
1055 28 prior to the 2nd boost (A–F), and day 42 (G–L). (A, G) Anti-RBD IgG, (B, H) IgG1, (C, I)
1056 IgG2a, (D, J) IgG2a/IgG1 ratio, (E, K) hACE2/RBD inhibition rate, and (F, L) neutralizing titer
1057 were assessed. N=9–10 per group. Data were combined from two individual experiments and
1058 analyzed by one-way ANOVAs followed by post-hoc Tukey's test for multiple comparisons. (M)
1059 Splenocytes were collected 2 weeks after the final immunization and stimulated with a SARS-
1060 CoV 2 Spike peptide pool in the presence of anti-CD28 antibody (1 µg/mL). After 24 (for IL-2
1061 and IL-4) and 96 (for IFN γ) hours, supernatants were harvested and cytokine levels were
1062 measured by ELISA. N=4-5 per group. Data were log-transformed and analyzed by one-way
1063 ANOVAs followed by post-hoc Tukey's test for multiple comparisons. * $P < 0.05$, ** $P < 0.01$,
1064 *** $P < 0.001$, **** $P < 0.0001$. Blue and red colored asterisks respectively indicate comparisons
1065 to RBD and AH adjuvanted RBD groups. Box-and-whisker plots represent the minimum, first
1066 quartile, median, third quartile, and maximum value. LLD, lower limit of detection.



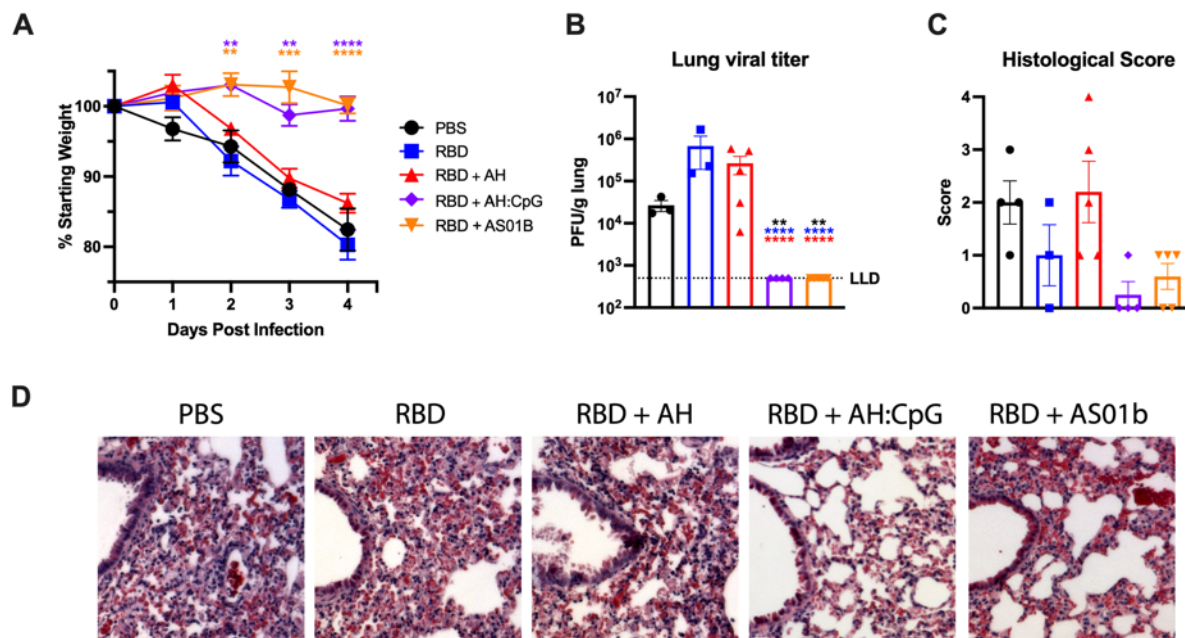
1067

1068 **Figure 3. SARS-CoV-2 challenge model of young and aged mouse recapitulates human age-**
 1069 **specific pathogenesis**

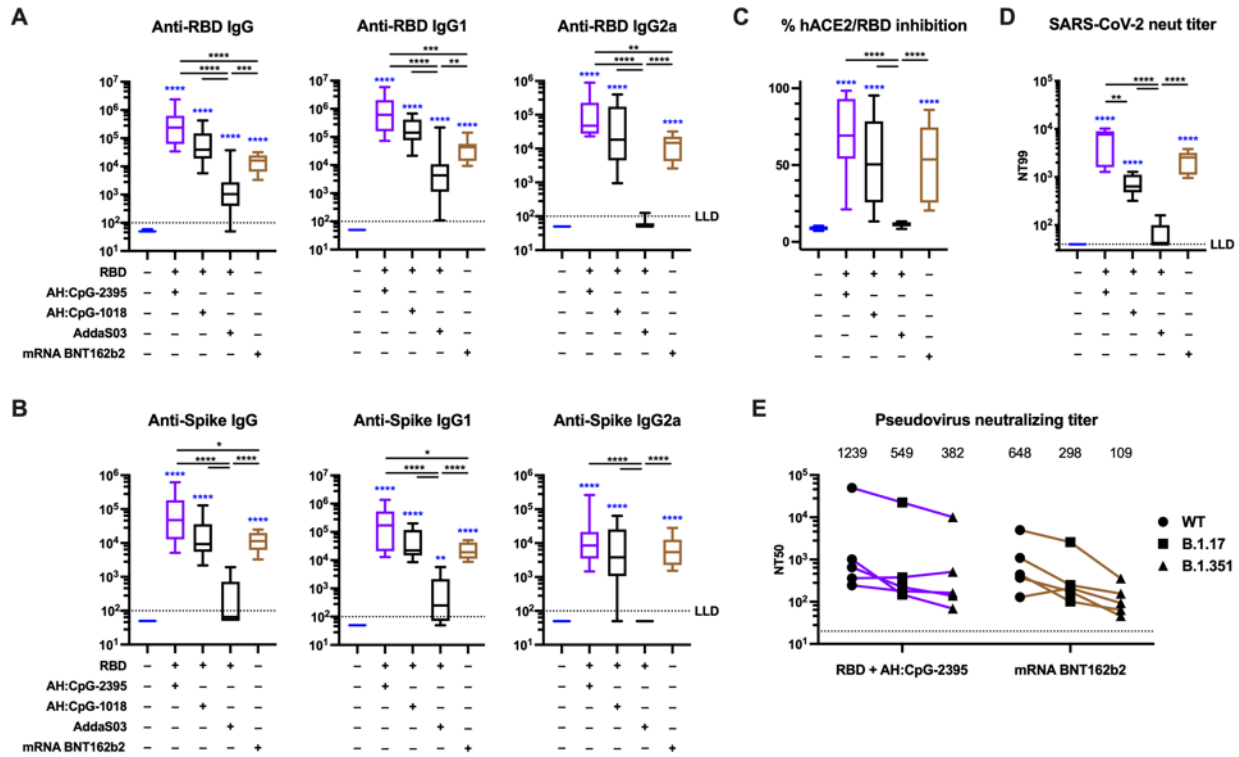
1070 Young (3-month-old) and aged (14-month-old) naïve BALB/c mice were challenged IN with
 1071 mock (PBS), or 10², 10³, 10⁴, and 10⁵ PFU of mouse-adapted SARS-CoV-2 (MA10).

1072 Bodyweight change of (A) young adult and (B) aged mice were assessed daily up to 4 days post
 1073 infection. Data represent mean and SEM with body weights only shown for surviving mice at

1074 each time-point. Data were analyzed by one-way ANOVA followed by Dunnett's test for
1075 comparisons against the PBS group. (C) Survival rate of aged mice. Data were analyzed by log-
1076 rank test in comparison to PBS group. (D) Viral titer in lung homogenates at 4-days post SARS-
1077 CoV-2 challenge (young: n=5 per group, aged: n=5 for 10^2 ; n=4 for 10^3 ; n=1 for 10^4 ; and n=0 for
1078 10^5). Results represent mean \pm SEM. (E) Representative lung histological images at 4-days post
1079 challenge. H&E is shown. * $P < 0.05$, ** $P < 0.01$, *** $P < 0.001$, **** $P < 0.0001$.



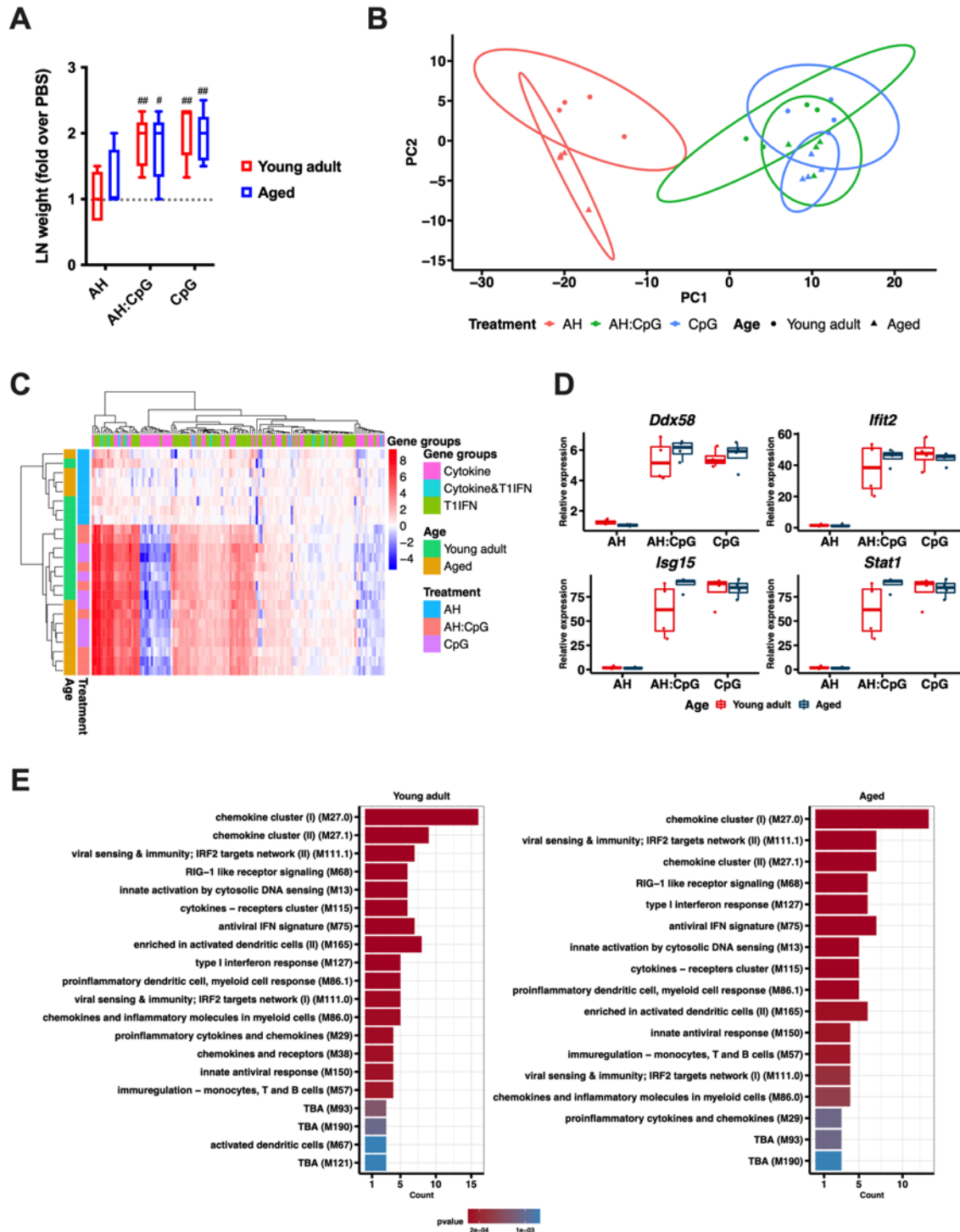
1080
 1081 **Figure 4. AH:CpG-adjuvanted vaccine protects aged mice from SARS-CoV-2 challenge**
 1082 Aged, 14-month-old BALB/c mice were immunized as in **Figure 2**. On Day 70 (6 weeks post 2nd
 1083 boost), mice were challenged IN with 10³ PFU of mouse-adapted SARS-CoV-2 (MA10). **(A)**
 1084 Bodyweight changes were assessed daily up to 4 days post infection. Data represent mean and
 1085 SEM with body weights shown for surviving mice at each time-point (one mouse in RBD group
 1086 died at 4 days post infection). Data were analyzed by one-way ANOVA followed by Dunnett's
 1087 Test for comparisons between PBS group. **(B)** Viral titer in lung homogenates at 4-days post
 1088 SARS-CoV-2 challenge. Results represent mean \pm SEM. Data were analyzed by one-way
 1089 ANOVA followed by post-hoc Tukey's test for multiple comparisons. ** $P < 0.01$, **** P
 1090 < 0.0001 . Black, blue and red colored asterisks respectively indicate comparisons to PBS, RBD,
 1091 and RBD + aluminum hydroxide (AH) groups. LLD, lower limit of detection. **(C)** Lung
 1092 interstitial inflammation was evaluated and converted to a score of 0-4 with 0 being no
 1093 inflammation and 4 being most severe. **(D)** Representative lung histological images at 4-days
 1094 post challenge. H&E is shown. N=4-5 animals per group.



1095
1096 **Figure 5. AH:CpG-adjuvanted RBD vaccines and an authorized spike mRNA vaccine elicit**

1097 **comparable levels of neutralizing antibodies in aged mice**

1098 Aged, 14-month-old BALB/c mice were immunized IM on Days 0 and 14 with monomeric
1099 SARS-CoV-2 RBD protein with indicated adjuvants, or BNT162b2 Spike mRNA vaccine as
1100 described in Methods. Serum samples were collected and analyzed on Day 28. (A) Anti-RBD
1101 binding ELISA, (B) anti-Spike binding ELISA, (C) hACE2/RBD inhibition rate, and (D) SARS-
1102 CoV-2 virus neutralizing titer were assessed. N=9–10 per group. Data were combined from two
1103 individual experiments and analyzed by one-way ANOVAs followed by post-hoc Tukey's test
1104 for multiple comparisons. (E) Pseudovirus neutralizing titers against wild-type or the B.1.17 or
1105 B.1.351 variants were assessed. N=5 per group. The numbers indicate GMT. Each symbol
1106 represents an animal. * $P < 0.05$, ** $P < 0.01$, *** $P < 0.001$, **** $P < 0.0001$. Blue colored asterisks
1107 indicate comparisons to PBS group. Box-and-whisker plots represent the minimum, first quartile,
1108 median, third quartile, and maximum value. LLD, lower limit of detection.



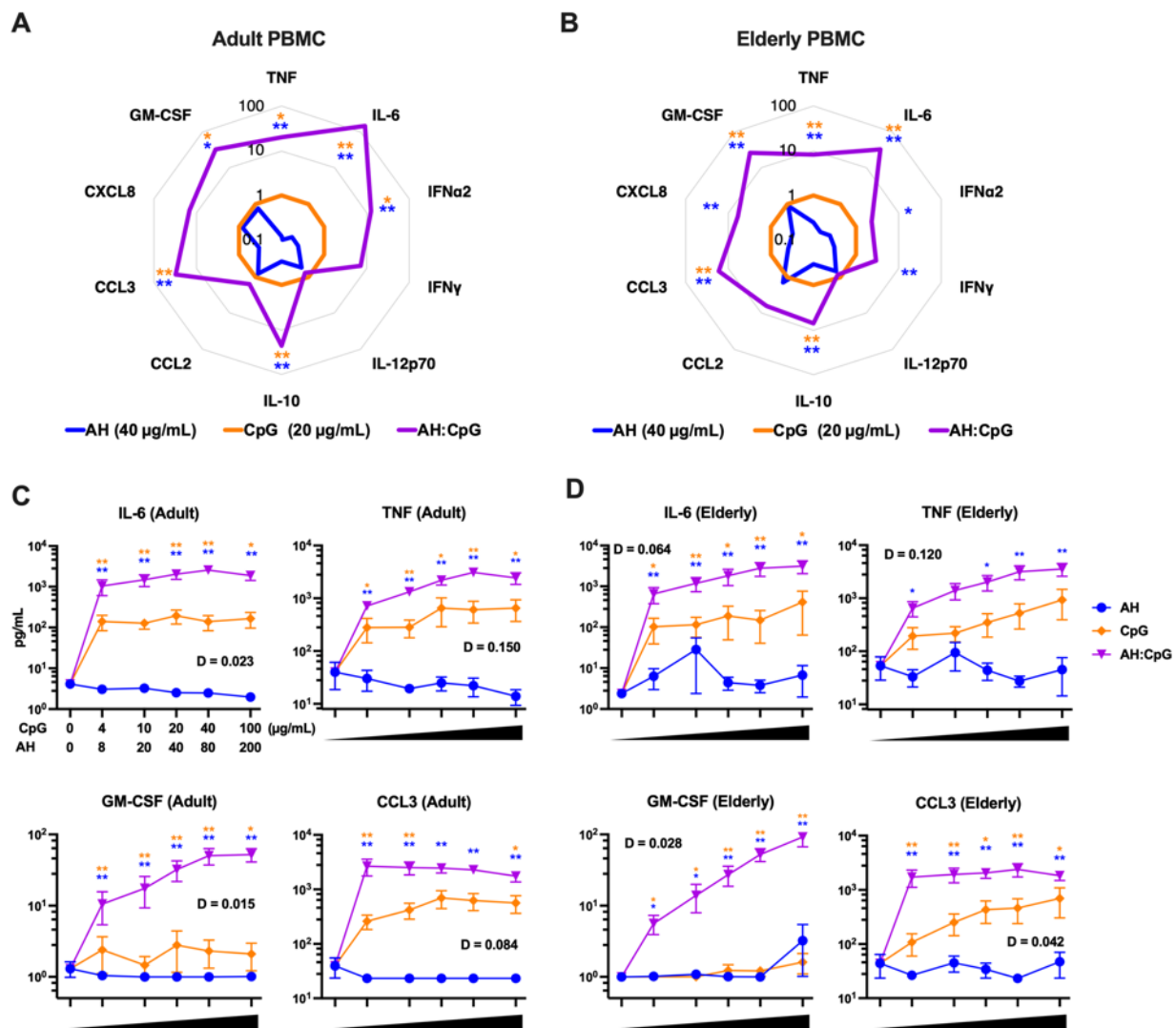
1109

1110 **Figure 6. AH:CpG elicits comparable lymph node innate responses in young and aged mice**

1111 Young (3-month-old) and aged (14-month-old) mice were subcutaneously injected with

1112 aluminum hydroxide (AH), CpG, or AH:CpG. 24 hours later, draining lymph nodes (dLNs) were

1113 collected and RNA was extracted. **(A)** Weights of dLNs were measured and expressed as fold
1114 over contralateral, PBS-injected LN. N=5 per group. # and ## respectively indicate $P < 0.05$ and
1115 0.01 when comparing each group against the value 1 (which represents the contralateral control
1116 sample expressed as fold). **(B–E)** RNA isolated from dLNs was subjected to a quantitative real-
1117 time PCR array comprised of 157 genes related to cytokines, chemokines, and type 1 IFN
1118 responses. N=4 animals per group. **(B)** Principal component analysis demonstrated a marked
1119 separation by treatment and age. **(C)** Unsupervised hierarchical clustering revealed major
1120 differences between treatments and highlighted the marked difference between AH and CpG-
1121 containing treatments. Each column represents gene categories and rows represent samples. **(D)**
1122 Generalized linear model comparing treatment and age with each gene was performed. The top 4
1123 significant genes (*Ddx58*, *Ifit2*, *Isg15*, *Stat1*) were selected and plotted with their relative
1124 expression values by age and treatment. Statistical analysis of the plots employed the Kruskal-
1125 Wallis test to compare mean differences across groups and Wilcoxon test to compare between
1126 ages. **(E)** Enrichment analysis of differentially expressed genes using the blood transcriptional
1127 modules (Li et al., 2013- PMC: 24336226) was performed from the significant gene results after
1128 the generalized linear model by treatment. The top 20 modules are summarized per age.

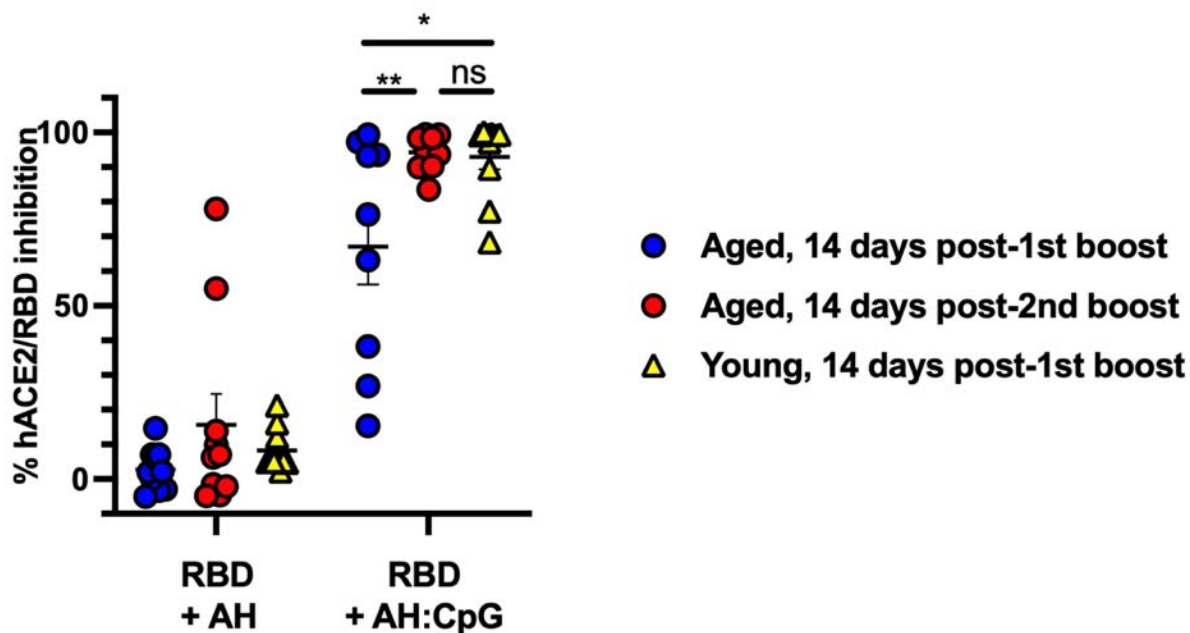


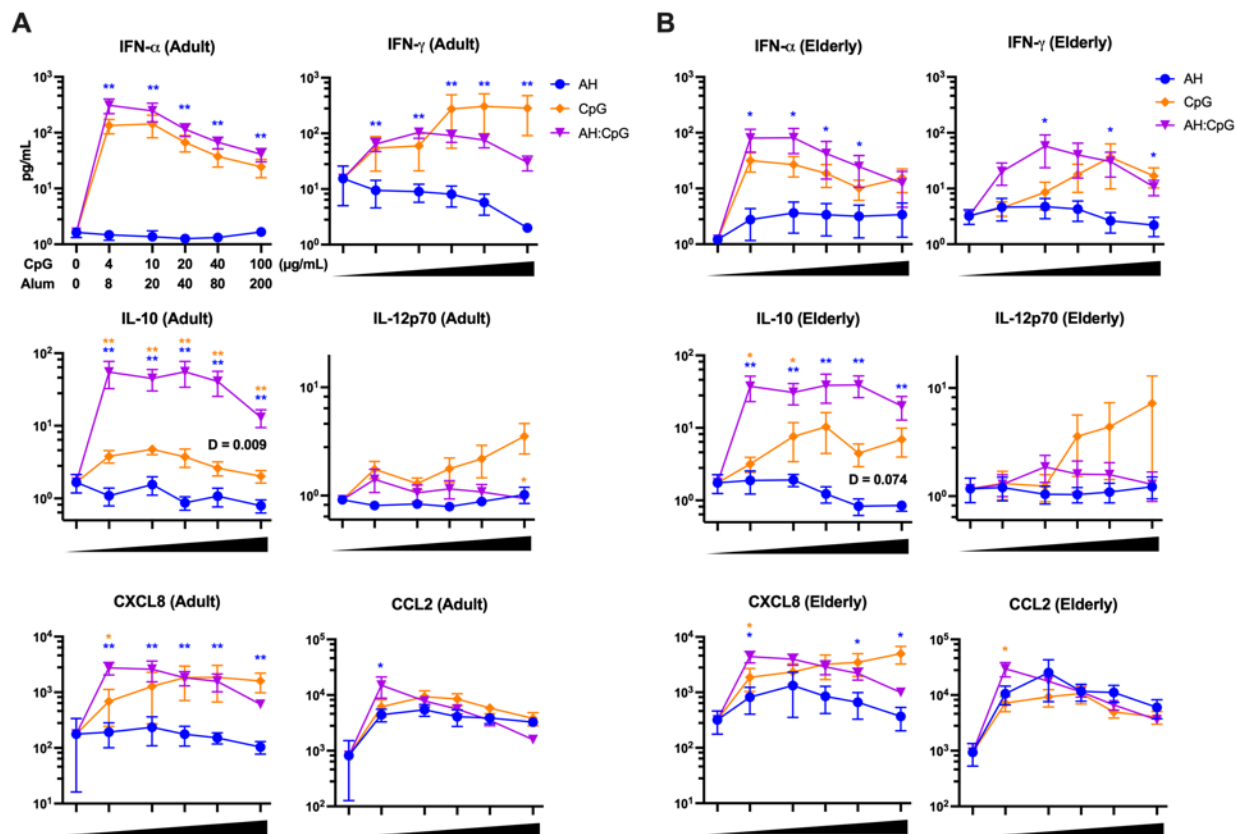
1129
 1130 **Figure 7. AH:CpG synergistically enhances proinflammatory cytokine production from**
 1131 **human adult and elderly PBMCs**

1132 Human PBMCs collected from young adult (**A, C**) and elderly individuals (**B, D**) were cultured
 1133 *in vitro* for 24 h with CpG alone (4, 10, 20, 40, and 100 $\mu\text{g/mL}$), aluminum hydroxide (AH)
 1134 alone (8, 20, 40, 80, and 200 $\mu\text{g/mL}$), or a combination of both. Supernatants were collected for
 1135 multiplexing bead array. N=6 per age group. (**A-B**) Radar plot analysis of cytokines and
 1136 chemokines are presented as a fold-change over the CpG alone group for the 20 $\mu\text{g/mL}$ CpG and
 1137 40 $\mu\text{g/mL}$ AH conditions. (**C-D**) Results represent mean \pm SEM. Unpaired Mann-Whitney tests
 1138 were applied at each concentration. Blue and yellow colored asterisks indicate comparisons of

1139 AH:CpG formulation to AH and CpG alone groups, respectively. * $P < 0.05$, ** $P < 0.01$. Level of
1140 synergy was calculated using an adapted Loewe definition of additivity ($D < 1$: synergy, $D = 1$:
1141 additivity, $D > 1$: antagonism).

1142 SUPPLEMENTARY MATERIALS





1154

1155 **Supplementary Figure 2. AH and CpG synergistically induce cytokine and chemokine**
 1156 **production by human young adult and elderly PBMCs**

1157 Human PBMCs collected from young adults (A) and elderly individuals (B) were cultured *in*
 1158 *vitro* for 24 hrs with CpG alone (4, 10, 20, 40, and 100 $\mu\text{g/mL}$), aluminum hydroxide (AH) alone
 1159 (8, 20, 40, 80, and 200 $\mu\text{g/mL}$), or combinations of each. Supernatants were collected for
 1160 multiplexing bead array. N=6 per age group. Unpaired Mann-Whitney tests were applied at each
 1161 concentration. Level of synergy was calculated using an adapted Loewe definition of additivity
 1162 ($D < 1$: synergy, $D = 1$: additivity, $D > 1$: antagonism). D value was not calculated if the
 1163 concentration-dependent cytokine level did not fit a linear regression curve. Blue and yellow
 1164 colored asterisks indicate comparisons of AH:CpG formulation to AH and CpG alone groups,
 1165 respectively. Results represent mean \pm SEM. * $P < 0.05$, ** $P < 0.01$.